Controls on connectivity and streamflow generation in a Canadian Prairie landscape

A Thesis Submitted to the
College of Graduate Studies and Research
In Partial Fulfillment of the Requirements
For the Degree of Master of Environment and Sustainability
In the School of Environment and Sustainability
University of Saskatchewan
Saskatoon, Canada

By

Rosa Elizabeth Brannen

PERMISSION TO USE

In presenting this thesis in partial fulfillment of the requirements for a Postgraduate degree from the University of Saskatchewan, I agree that the Libraries of this University may make it freely available for inspection. I further agree that permission for copying of this thesis in any manner, in whole or in part, for scholarly purposes may be granted by the professor or professors who supervised my thesis work or, in their absence, by the Head of the Department or the Dean of the College in which my thesis work was done. It is understood that any copying or publication or use of this thesis or parts thereof for financial gain shall not be allowed without my written permission. It is also understood that due recognition shall be given to me and to the University of Saskatchewan in any scholarly use which may be made of any material in my thesis.

DISCLAIMER

Reference in this thesis to any specific commercial products, process, or service by trade name, trademark, manufacturer, or otherwise, does not constitute or imply its endorsement, recommendation, or favoring by the University of Saskatchewan. The views and opinions of the author expressed herein do not state or reflect those of the University of Saskatchewan, and shall not be used for advertising or product endorsement purposes.

Requests for permission to copy or to make other uses of materials in this thesis in whole or part should be addressed to:

Head of the School of Environment and Sustainability
University of Saskatchewan
Saskatoon, Saskatchewan S7N 5C8
Canada

OR

Dean
College of Graduate Studies and Research
University of Saskatchewan
107 Administration Place
Saskatoon, Saskatchewan S7N 5A2
Canada

ABSTRACT

Linkages between the controls on depressional storage and catchment streamflow response were examined in a wetland dominated basin in the Canadian Prairie Pothole region through a combination of field monitoring and modelling. Snowmelt, surface storage, water table elevation, atmospheric fluxes, and streamflow were monitored during spring snowmelt and summer in a 1 km^2 sub-catchment containing a semi-permanent pond complex connected via an intermittent stream. Snow accumulation in the basin in spring of the 2013 study year was the largest in the 24-year record. Rainfall totals in 2013 were close to the long term average, though June was an anomalously wet month. The water budget of the pond complex indicates that there was a significant subsurface contribution to surface storage, in contrast to previous studies in this region. Following snowmelt, subsurface connectivity occurred between uplands and the stream network due to activation of the effective transmission zone in areas where the water table was located near the ground surface, allowing significant lateral movement of water into the stream network. Modelling results suggest there was significant infiltration into upland soils during the study period and that upland ponds are an important consideration for accurately simulating catchment discharge. The flux of groundwater to the wetland complex during periods of subsurface connectivity was also important for maintaining and re-establishing surface connectivity and streamflow. As the observed period of surface and subsurface hydrological connectivity was one of the longest on record in the catchment due to very wet conditions, the results of this study denote observations of the wet extremes of the hydrological regime important for proper understanding, modelling, and prediction of streamflow in the region.

ACKNOWLEDGEMENTS

I wish to express my deepest gratitude and appreciation to the many people whose guidance and support have made this thesis possible. I would first like to thank my supervisors Dr. Chris Spence and Dr. Andrew Ireson for their encouragement and expertise. Chris always made time to provide advice and discuss ideas. Thanks for his patience, mentorship, and sense of humour. I give my heartfelt thanks to Andrew for his perspective, invaluable feedback, and enthusiasm. It was a pleasure to work with them both. I am grateful to the other members of my thesis committee, Dr. Jeff McDonnell, Dr. Cherie Westbrook, and Dr. Christy Morrissey and external examiner, Dr. Lawrence Martz, for their time, helpful suggestions, and assurance along the way.

I would also like to thank those people who provided field and technical support during this project. Thanks to Randy Schmidt and Dr. Garth van der Kamp for their valuable assistance in the field, extensive knowledge of the site, and for providing essential data. The logistical support of Heather Wilson was much appreciated. Samson Mengistu, Anna Coles, Newell Hedstrom, and Dell Bayne were very helpful in the field and generously contributed their time and equipment to this project.

I am particularly grateful to have been part of such a wonderful community at the Global Institute for Water Security. Special thanks to my lab group for their advice and interest in my work. This would not have been nearly as an enjoyable experience without the lunches and laughter shared with my fellow students. I was lucky to have such a supportive group of peers including Anna, Kathryn, Meghan, Raea, Noel, Amber, and many others.

Finally, I thank my friends and family for their years of love and support. I am grateful to my partner, Ty, who has experienced all the highs and lows of my research. I could not have

finished this work without his daily encouragement, his companionship, and his ability to make me laugh. To my parents, who never let me doubt myself, thank you for tirelessly supporting me through all of life's adventures.

This project would not have been possible without the financial contributions of the following organizations: Canada Excellence Research Chair in Water Security, School of Environment and Sustainability, Environment Canada (Lake Winnipeg Basin Initiative), and the Natural Sciences and Engineering Research Council.

TABLE OF CONTENTS

LIST OF TABLES

LIST OF FIGURES

LIST OF SYMBOLS

a	Pond drainage constant [$m^2\ d^{-1}$]
A_p	Pond surface area [m^2]
a_s	Snow covered area [m^2]
b	Pond drainage exponent [-]
c_p	Specific heat [MJ kg^{-1} $^oC^{-1}$]
d	Snow depth [mm]
D	Vapour pressure deficit [kPa]
DEM	Digital Elevation Model
E	Open water evaporation [mm d^{-1}]
f	Snowmelt infiltration capacity [mm d^{-1}]
f*	Infiltration capacity [mm d^{-1}]
FC	Field capacity [m]
G	Net groundwater exchange [mm d^{-1}]
h	Stage [m]
h_p	Pond stage [m]
h_T	Pond spill threshold [m]
J_w	Change in heat storage [MJ m^{-2} d^{-1}]
K_s	Saturated hydraulic conductivity [m d^{-1}]
L	Hillslope length [m]
LCA	Land cover class
LiDAR	Light detection and ranging
M	Snowmelt [mm d^{-1}]
M_a	Ablation [mm d^{-1}]
p	Pond profile coefficient [-]
P_d	Direct precipitation [mm d^{-1}]
q	Water vapour density [g m^{-3}]
Q	Discharge [$m^3\ s^{-1}$]
Q^*	Net radiation [MJ m^{-2} d^{-1}]
Q_e	Latent heat flux [W m^{-2}]
Q_e	Event streamflow [$m^3\ d^{-1}$]
Q_i	Inflow [mm d^{-1}]
Q_o	Outflow [mm d^{-1}]
Q_S	Simulated streamflow [$m^3\ d^{-1}$]
R	Surface runoff [mm d^{-1}]
r_a	Aerodynamic resistance [d m^{-1}]
RH	Relative humidity [%]
RMSE	Root mean square error
r_S	Overland flow from upland ponds [mm d^{-1}]

r_M	Infiltration excess snowmelt runoff [mm d^{-1}]
r_R	Infiltration excess rainfall runoff [mm d^{-1}]
s	Pond shape coefficient [m2]
S_b	Sublimation [mm d^{-1}]
Ss_0	Initial soil moisture deficit [m]
S_T	Total reach storage [mm]
SWE	Snow water equivalent [mm]
S_y	Specific yield [-]
T	Transmissivity [m^2 d^{-1}]
t^*	Recession coefficient [d]
T_a	Air temperature [°C]
T_s	Surface water temperature [°C]
T_W	Water temperature [°C]
u	Wind speed [m s^{-1}]
u_{dir}	Wind direction [°]
V_p	Pond volume [m^3]
w	Pond circumference [m]
z	Depth [m]
α_M	Snowmelt runoff partitioning ratio (-)
α_R	Rainfall runoff partitioning ratio (-)
γ	Psychometric constant [kPa °C^{-1}]
Δ	Slope of the sat. vap. press. temp. relationship [kPa °C^{-1}]
Θ_P	Pore saturation [%]
λ	Latent heat of vapourization [MJ kg^{-1}]
ξ	Residual [mm d^{-1}]
ρ_a	Air density [kg m^{-3}]
ρ_S	Snow density [kg m^{-3}]
ρ_W	Water density [kg m^{-3}]

CHAPTER 1 : INTRODUCTION

The Prairie Pothole Region (PPR) of North America is a landscape characterized by millions of glacially formed topographic depressions, many of which contain wetlands. Wetlands are areas of the landscape that have saturated or nearly saturated soil most of the year, and have a fixed area, which is defined by hydric soils and hydrophytes (Stewart and Kantrud, 1971). Wetlands may contain ponds, which refers to the variably flooded portion of the wetland (van der Kamp and Hayashi, 2009). Both the expansion of stream networks that form between wetland ponds and streamflow production within them are very strongly threshold-mediated, determined by the storage capacity of wetlands, which can limit the area contributing runoff to the catchment outlet (Leibowitz and Vining, 2003; Shaw et al., 2012). Predicting the occurrence and magnitude of streamflow events is complicated by these storage thresholds and the non-linearity in storage-discharge relationships in wetland-dominated basins (Shook and Pomeroy, 2011; Shaw et al., 2012). The water budget of ponds is a dominant control on pond to pond connectivity, the emergence of intermittent stream networks, and streamflow generation at large basin scales. Sound water resource prediction is important in this region because the vitality of the economy is very much dependent on water and is vulnerable to changes in climate. The floods of 2007, 2011, and 2013 on the Prairies and the consequent costs to the economy have drawn attention to the necessity of developing a better understanding of the controls that dictate storage, connectivity, and stream discharge in the region.

Studies of the hydrological functioning of prairie wetlands to date have been fairly dichotomous, emphasizing either groundwater or surface water. Early research focused on the importance of groundwater in controlling the chemistry of ponds (e.g., Hayashi et al., 1998b; LaBaugh et al., 1987), and its effect on the stability of wetland ponds during periods of drought

(LaBaugh et al., 1996; Winter and Rosenberry, 1998; Winter, 2000). More recently, there has been a shift towards explaining prairie wetland hydrology and chemistry from the perspective of streamflow and the importance of surface water connections in governing both the water level of ponds and the streamflow response in wetland dominated basins (Leibowitz and Vining, 2003; van der Valk, 2005; Cook and Hauer, 2007; Shaw et al., 2012). This is part of a paradigm shift in which hydrologists are recognizing that runoff generation is a threshold-mediated process controlled by connectivity of multi-scale landscape, hillslope, or soil components (Tromp van-Meerveld and McDonnell, 2006; Spence, 2007; Spence, 2010; McNamara et al., 2011; Seibert et al., 2011). In the context of streamflow generation in the prairies, previous studies have either assumed that groundwater is negligible (Shook and Pomeroy, 2011), or that it is a loss pathway for transpiration from the riparian zone (Hayashi et al., 1998a). The goal of this thesis is to explore whether shallow groundwater systems in the prairies could provide a significant transmission pathway for water into ponds. The hypothesis to be tested is that groundwater discharge into ponds is a significant component of the pond water budget and groundwater-surface water exchanges are significant in sustaining pond to pond connectivity and streamflow.

The next chapter will be a literature review of previous work on dominant hydrological processes and streamflow generation in the Prairie Pothole Region along with modelling approaches for prairie basins. The research questions are also presented in Chapter 2. The study site is described in Chapter 3 and field and modelling methods in Chapter 4. Chapter 5 examines the dynamics of shallow groundwater-surface water interactions and hydrological connectivity in a sub-catchment of the PPR. Chapter 6 explores how a quantitative hydrological model can be used to simulate wetland water budgets and streamflow. Chapter 7 synthesizes the findings of this thesis.

CHAPTER 2 : LITERATURE REVIEW

This literature review will present a summary of Prairie Pothole Region hydrology, including surface and subsurface hydrological processes, their influence on depressional storage, the relation of storage to hydrological connectivity and non-linear runoff responses, and current modelling approaches for prairie basins.

2.1 Prairie hydrology

In the semi-arid prairies potential evaporation generally exceeds precipitation. This, in combination with the low relief and relatively recent deposition of underlying glacial till, limits the volume of runoff and the development of a well-organized permanent stream network. Many wetlands are located in closed basins that lack inflow and/or outflow streams, and thus have a water budget controlled by snowmelt runoff and snow redistribution from surrounding uplands, evapotranspiration, and shallow groundwater exchange (Woo and Rowsell, 1993; Winter and Rosenberry, 1995; Hayashi et al., 1998a; LaBaugh et al., 1998) (Figure 2.1). The surface hydrology of prairie ponds depends largely on spring snowmelt. Snow transport forms snow drifts in prairie wetlands and contributes to high spring water levels (Fang and Pomeroy, 2008), and snowmelt on uplands is partitioned into snowmelt runoff, which can contribute significant volumes to wetland storage, and infiltration into underlying soil (Woo and Rowsell, 1993). The partitioning between runoff and infiltration depends mainly on the infiltration capacity of frozen soils during snowmelt (Granger et al., 1984; Woo and Rowsell, 1993). The degree of infiltration into frozen soil can be restricted, limited, or unlimited depending on antecedent soil moisture and the presence of macropores, cracks, and ice lenses (Granger et al., 1984; Hayashi et al., 2003, van der Kamp et al., 2003).

Restricted infiltration describes the case where an impeding layer at the surface or within the soil zone completely prevents the downward movement of water. Limited infiltration describes the case of infiltration into uncracked soils without an impeding layer. The degree to which infiltration is limited in frozen soils is related to moisture content, due to the reduction in hydraulic conductivity caused by constriction and blockage of water by ice-filled pores (Granger, et al., 1984). Unlimited infiltration can occur in heavily cracked soils, which are usually heavy clays where cracks form following hot, dry conditions in the growing season (Granger et al., 1984). The infiltrability of frozen soil is much greater in grass than cultivated fields as undisturbed cover leads to the development of macropore networks. Runoff is correspondingly smaller from brush and tall grass than cultivated fields (van der Kamp et al., 2003). Zhao et al. (1997) demonstrated that in unsaturated frozen soil, initial infiltration into frozen soils can fill air-filled pore space. This may result in a relatively rapid infiltration rate until infiltrating water refreezes, which blocks deeper flow. The thawing front, or the depth of the frost table, acts as a moving impermeable boundary. The downward movement of the thawing front requires energy input from the surface, through conduction from upper soil layers. When the thawing front breaks through the frozen soil layer, there can be an increase in infiltration rate and response of the water table. Hayashi et al. (2003) found that the advance of the thawing front is slower under uplands than in depressions because the energy input is lower. Standing water in depressions traps incoming radiation and conducts it into the soil more effectively than soil on uplands, leading to shallow groundwater recharge beneath the depression (Hayashi et al., 2003). Snowmelt runoff over frozen soils and direct precipitation are generally the main inputs to prairie wetlands in closed basins (Woo and Rowsell, 1993), as most summer precipitation on uplands

infiltrates into the soil and is consumed by evapotranspiration within the root zone without recharging shallow groundwater (Hayashi et al., 1998a).

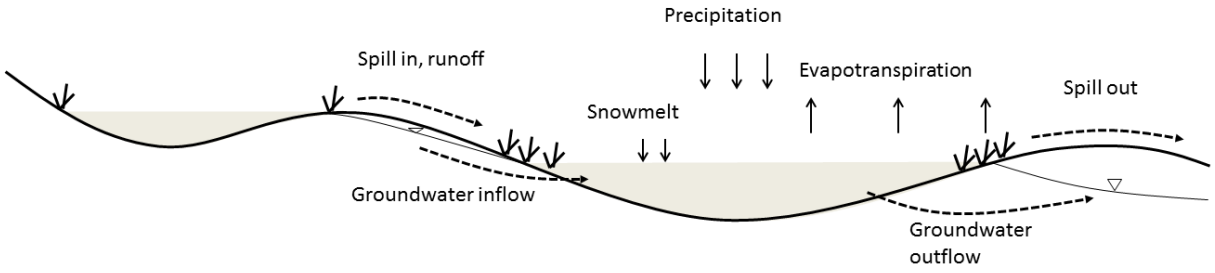

Figure 2.1: Simplified diagram depicting water budget components of a prairie wetland. Dashed arrows indicate fluxes that are dependent on the degree of surface and/or subsurface storage (modified from van der Kamp and Hayashi, 2009).

The hydraulic conductivity of the glacial till underlying much of the prairies increases exponentially in the near surface, due to fracturing and macropores caused by weathering (van der Kamp and Hayashi, 2009). As a result of this characteristic, the greatest subsurface flows occur within the saturated zone when the water table is near the ground surface (Hayashi et al., 1998a; van der Kamp and Hayashi, 2009). For groundwater flow to be significant to the water budget of ponds it must be shallow, within 5-6 meters of the surface, due in most part to the exponential increase in hydraulic conductivity near the surface (van der Kamp and Hayashi, 2009). Deeper, regional groundwater flow into or out of small catchments is usually not significant due to the low hydraulic conductivity of clay-rich glacial till deposits (Hayashi et al., 1998a).

Surface and subsurface hydrological processes are intrinsically linked in this region, especially when the water table is close to the surface. One example is pond recession driven by lateral subsurface flow away from the wetland due to evapotranspiration from vegetation along the wetland margin (van der Kamp and Hayashi, 2009). This notwithstanding, it has been proposed that temporary surface hydrological connectivity between wetlands may also be an important control on the hydrology and chemistry of prairie potholes and on runoff from larger watersheds across the region (Leibowitz and Vining, 2003; Shaw et al., 2012).

Hydrological connectivity, defined as a measure of the ability to transfer water from one part of a landscape to another (Bracken and Croke, 2007), has proven a useful concept in explaining variations in hillslope runoff response in a range of different environments (Devito et al., 1996; McGlynn and McDonnell, 2003; Buttle et al., 2004). Recent work has emphasized the importance of interactions between variable hydrologic pathways and source areas in headwater catchments to watershed scale hydrologic response. At the hillslope scale, hydrological connectivity will vary with the dynamics of saturation excess overland flow (Dunne and Black, 1970), or the topographically controlled fill-and-spill runoff mechanism (Spence and Woo, 2003). At the catchment scale, surface-groundwater connectivity has been shown to be a dominant control on the magnitude and timing of observed streamflow (Sidle et al., 2000; Jencso et al., 2009). Surface-groundwater connectivity is achieved when the saturated zone below the water table is located within a transmissive zone and there is a continuous hydraulic gradient from the hillslopes, through the riparian zone, and into the stream. Investigating how storage capacities in heterogeneous stores are exceeded across the landscape and hydrologically connect among each other to produce connected flow paths to the stream has been suggested as an

approach to understanding emergent hydrological behaviour of catchments across a variety of environments and scales (Bracken et al., 2013).

In prairie basins, wetland depressions have a significant effect on basin discharge, as they play a considerable part in determining surface hydrological connectivity and control the proportion of the basin that contributes to the outlet (Shaw et al., 2012). Both the size of the runoff event and the antecedent conditions determine where storage capacity is reached (Shaw et al., 2012). To determine when and where depressional storage thresholds will be exceeded it must be understood how the volume of surface water storage in depressions changes over time due to interactions with groundwater, surface water, and atmospheric water. Streams in the prairie pothole region show little in the way of baseflow (Shook and Pomeroy, 2011); lacking is an understanding of how interactions between shallow groundwater and ponds may influence surface connectivity between wetlands.

The water budget of wetlands in the prairie region is extremely variable and wet and dry episodes are characteristic of this region (LaBaugh et al., 1998). Drier years produce storage deficits, while wet years produce a storage surplus (Woo and Rowsell, 1993). Extended wet periods are likely to produce longer term positive imbalances in the water budget that can increase the number, density, and total surface area of prairie wetlands (LaBaugh et al., 1998). Long term water-level studies in the PPR have shown that oscillatory water-level fluctuations have occurred for thousands of years and will likely continue to occur in the future (van der Valk, 2005). The prairies have recently been experiencing wetter than average conditions, which presents an opportunity to conduct a water budget study during a period of extensive connectivity to determine how this state of catchment wetness influences runoff.

2.2 Prediction/modelling

Modelling Canadian prairie hydrology has applications in flood forecasting and drought analysis, determining the effects of land-use change, assessing agricultural land, and water resource management. As soil moisture balance is of utmost importance to agricultural activities and is dominated by inputs of precipitation and losses from evaporation, many prairie modelling studies have focused on the processes of snow redistribution, accumulation, and melt (Fang and Pomeroy, 2009); infiltration into frozen soils (Zhao and Gray, 1999); and evaporation (Armstrong et al., 2008). More recently, there has been interest in modelling storage and streamflow in wetland dominated basins (Fang et al., 2010; Shook and Pomeroy, 2011; Huang et al., 2013).

The importance of the variation in connections between water stores across a multitude of scales to runoff production must be recognized when modelling prairie basins. The results of studies on storage and discharge relationships in this region suggest that storage thresholds are an important factor in accurately assessing runoff regimes (Spence, 2007; Shook and Pomeroy, 2011). The distribution of water must be accurately estimated to determine the contributing area to streamflow because surface connectivity of wetlands only occurs when wetlands are full, and the size of the runoff event and antecedent conditions will determine where storage is overwhelmed (Shook and Pomeroy, 2011; Shaw et al., 2012). To simulate the fill-and-spill behaviour of wetlands on a sub-basin scale, accurate wetland water budgets are required.

Several models have been developed for simulating wetland storage. Some studies have focused on large scale basins with a large degree of wetland storage (Vining, 2002; Fang et al., 2010; Shook and Pomeroy, 2011); where others have focused on using semi-distributed conceptual models to simulate the water budget of individual wetlands (Su et al., 2000;

Krasnostein and Oldham, 2004; Johnson et al., 2010). A common approach for determining dominant hydrological controls in a wetland environment is to calculate a water budget based on all the fluxes to the wetland (Woo and Rowsell, 1993; Hayashi et al., 1998a; Ferone and Devito, 2004). However, significant uncertainty exists in the magnitude of many of the fluxes, especially groundwater flow (van der Kamp and Hayashi, 2009). Even in studies where all components of the water budget are estimated, the results are specific to conditions occurring during the period of data collection. Numerical models for predicting groundwater flow (e.g. MODFLOW) can be used to predict groundwater flow input data required to close the wetland water budget, but these are complex with large data requirements (Harbaugh et al., 2000). These models are better suited to simulating steady state conditions or annual variations (Townley et al., 1993). In contrast, a conceptual model, such as used by Krasnostein and Oldham (2004) and Su et al. (2000), may be a flexible tool for understanding and predicting wetland hydrology.

Su et al. (2000) modified a semi-distributed streamflow model (SLURP) to calculate water storage in a single wetland. In this model, the pond was represented by a soil moisture bucket to which rainfall, runoff, and snowmelt were added, and evaporation was subtracted, with no outflow allowed from the wetland. This semi-distributed structure was adequate for representing water level fluctuations in a single wetland, but does not provide an explicit means to describe how wetlands contribute to streamflow and interact with each other and other water stores in the landscape. Similarly, Krasnostein and Oldham (2004) developed a model to simulate independently calculated components of the water budget by subdividing the wetland system into zones, or buckets. The model can be applied to quantify specific flows within and between catchments. The parameters that described the catchment, wetland, and fluxes between them were physically based on observations; thus the model required minimal calibration. The

authors concluded that this semi-distributed bucket approach was sufficient to isolate dominant hydrological processes in a wetland system and adequately simulate the dynamic groundwater – wetland surface water interactions that were observed. This may be a useful approach for developing quantitative conceptual models that are aimed at describing the interactions between ponds, catchments, and local groundwater.

Kirkby (1996) states that the primary function of models is as a qualitative thought experiment to test process conceptualizations, whereby first-order controls in hillslope hydrology can be explored using numerical experiments. Weiler and McDonnell (2004) suggest that to test conceptual models numerical hillslope models need to be robust enough to capture a variety of processes, but simple enough to be able to discern the effects of "tuning" a few different parameters on runoff dynamics. These experiments are not primarily concerned with developing a model to that can be fit or calibrated to observed data, but to provide a quantitative framework to replicate similar information to that observed in the field, while exploring different combinations of inputs and parameterizations of hillslope structure and how these affect dominant runoff mechanisms and processes.

2.3 Research questions

As described above, the current paradigm for streamflow generation on the prairies largely neglects subsurface processes, focusing on primarily snowmelt-surface runoff. One aspect that is lacking is an understanding and quantification of how subsurface processes influence surface storage in wetlands, surface connectivity, and streamflow dynamics. Due to above average precipitation inputs over the past several years, different hydrological responses are emerging in the region, including larger spring runoff events, longer streamflow recessions,

and more frequent rainfall runoff events. Therefore, this study will provide a baseline for further studies on the hydrology of prairie pothole catchments under such conditions that include robust water flux measurements. The goal of this thesis is to determine if subsurface flow is important for maintaining pond storage and, in turn, streamflow. To achieve this goal, both an intensive field study and modelling experiment will be undertaken. Specifically, the following research objectives will be addressed.

1. understand the relative roles of surface and subsurface storage on wetland water budgets
2. examine the controls on the dynamics of surface and subsurface hydrological connectivity and how these control streamflow response from a Prairie Pothole Region wetland complex
3. explore how a simple modelling experiment can simulate wetland storage and discharge from the study catchment.

CHAPTER 3 : STUDY SITE

The St. Denis National Wildlife Area (SDNWA) is located approximately 40 km east of Saskatoon (106° 5' 36" W, 52° 12' 34" N) in central Saskatchewan within the Prairie Pothole Region (Figure 3.1). The east section of the SDNWA contains the lower basin of a larger 10 km^2 catchment. The topography is moderately rolling hummocky terrain with slopes varying from 10-15% (Miller et al., 1985). Elevation varies between approximately 565 meters above sea level in the northwest portion of the study catchment to 546 meters above sea level in the major pond depressions. Field measurements focused on a reach of St. Denis Creek that flows one year in ten (Ehsanzadeh et al., 2012). The top of the study reach is bounded by a flume installed within an inlet channel near the northern border of the SDNWA. From there the channel flows south in a spill channel through a sequence of four large ponds (Pond 1, 125, 124 and 98), through a downstream flume and into Pond 90, which is the terminal pond of this basin (Figure 3.1), meaning that is has never spilled during the period of record. The gross catchment area between the two flumes is 1.2 km^2 and the area of the reach ponds is approximately 0.13 km^2. The four reach ponds are considered Class 4 and 5 wetlands, indicating that they contain semi-permanent to permanent ponds (Stewart and Kantrud, 1971). In addition to the ponds within the channel, the sub-catchment also contains many small Class 3 seasonal ponds, some of which contribute overland flow to the channel. There is a central upland plateau within the southern portion of the sub-catchment that has not contributed surface flow to the channel during the period of record (1970 to present).

Monthly mean temperatures are -19 °C in January and 18 °C in July. Long-term mean annual precipitation at SDNWA is 416 mm, of which 120 mm falls as snow (Environment Canada, 2012). Annual evaporation from large ponds and lakes in the surrounding area are

reportedly of the order of 700 mm (Parsons et al., 2004); however, measurements of evaporation from small ponds within the SDNWA are significantly less, approximately 200 – 300 mm (Hayashi et al., 1998a). Pond level data at SDNWA show that pond depth has a distinct annual cycle, which peaks during snowmelt period and declines during the summer months (Shaw et al., 2012). Pond depth records from Pond 90 and Pond 1 also show a decadal pattern influenced by atmospheric inputs (i.e., drought vs. deluge). Pond 1 spills in many years when it reaches the spill threshold (Figure 3.2). The water level regime of Pond 90 shows abrupt rises in stage during years that Pond 1 spills.

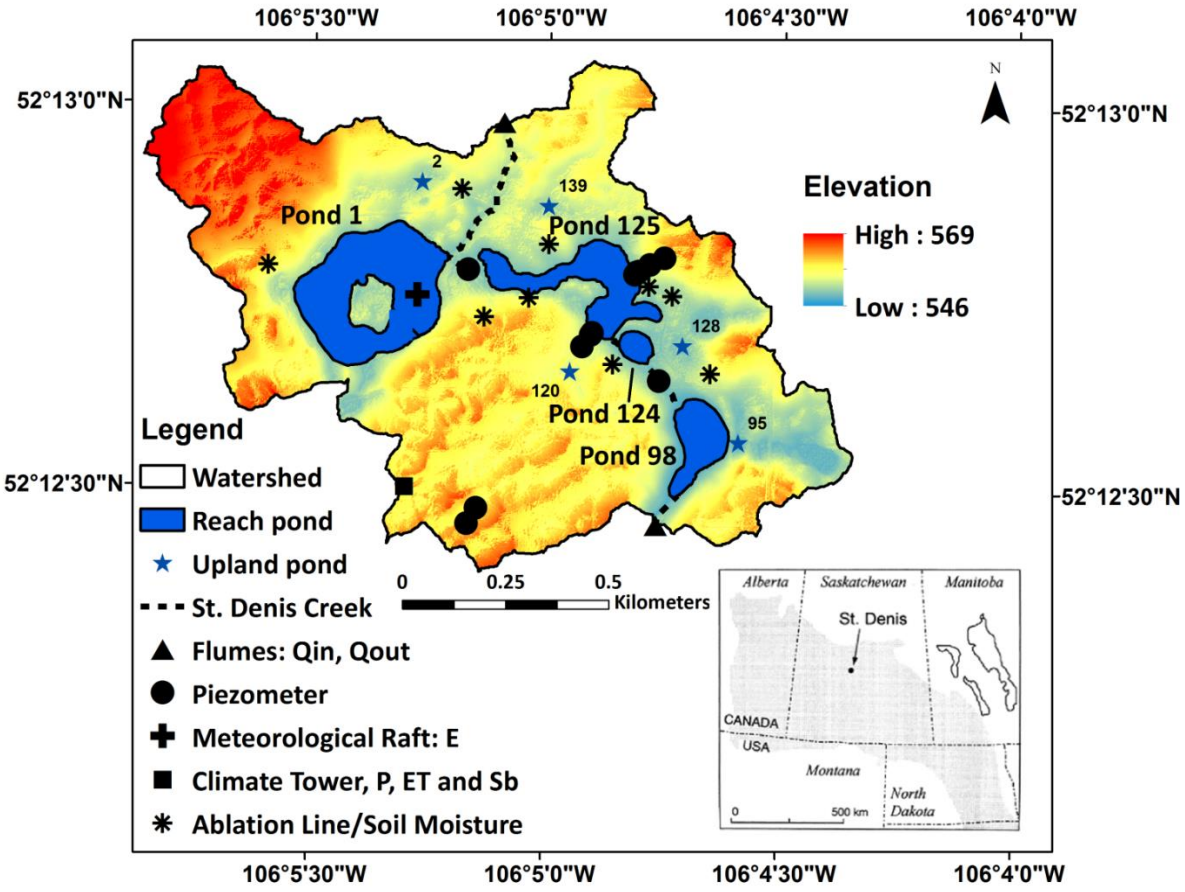

Figure 3.1: Study catchment and instrumentation with location map

Aspen bluffs, or "willow-rings", surround smaller ponds and some discrete areas around the larger ponds (Figure 3.3). The spill channel and the area directly adjacent to the spill channel

are untilled and covered by wetland vegetation. Native and non-native grasses cover 62% of the total study area in the north and east areas of the catchment. The areas south and west of Pond 1 are farmed; 11% of the study area is used for cultivating wheat (*Triticum spp.)* or canola (*Brassica spp.)*, and 5% of the area is currently bare soil. The remaining area is comprised of trees (7%) and open water (15%).

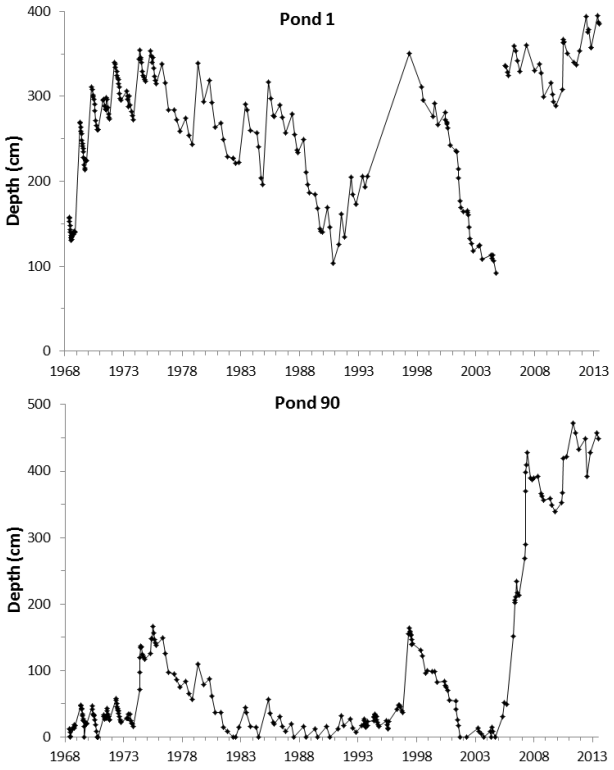

Figure 3.2: Pond level data at SDNWA, 1968–2013.

Slopes in the catchment are variable. The topography is steeper surrounding the major depressions (10-15%) than the smaller depressions in the uplands (2-10%). Slopes are steeper on the southern side of St. Denis Creek than the northern side. The difference in elevation between the two flumes is approximately 6 m (Figure 3.4). Aspect is an important control on snow redistribution and ablation processes in this landscape (Pomeroy and Gray, 1995). The aspect of hillslopes adjacent to the spill channel varies along the reach. Slopes adjacent to Pond 1 have

aspects that are mostly northeast and northwest, with a smaller area facing south and southeast. The slopes adjacent to Pond 125 are mainly of north and south-southwest aspect alongside the section of the pond that is oriented in a west-east direction; and northeast and west aspects beside the section that curves to the south. Pond 98 is located between slopes that are mainly facing east and northwest, with a smaller area facing south and southwest.

Figure 3.3: Landcover types: a) spill channel and wetland vegetation; b) bare soil, trees, and open water; c) grassed hillslope and open water.

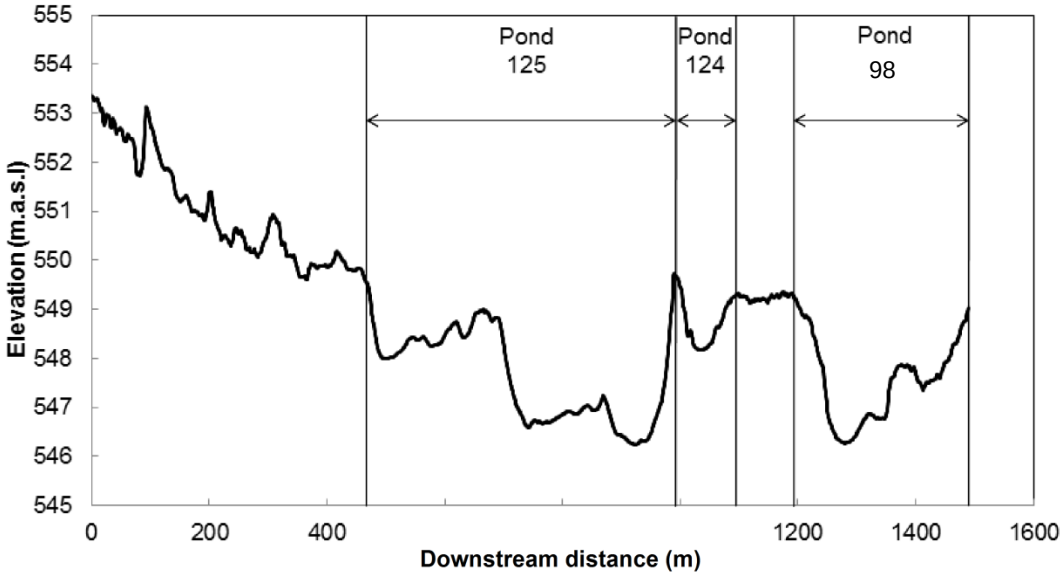

Figure 3.4: Longitudinal profile of the reach channel.

The soils are dominantly Orthic Dark Brown with significant Calcareous Dark Brown, Orthic Regosols, and Gleysolic soils, developed from medium to moderately fine-textured unsorted glacial till (Millar et al., 1985). The area is underlain by stratified silty glacio-lacustrine sediments that are further underlain by the glacial till of the Battleford and Floral formations (Hayashi et al., 1998a; Yates et al., 2006). The till is approximately 45% sand, 30% silt, and 25% clay (Miller et al., 1985) and has very low hydraulic conductivities, except for within discontinuous gravel or sand lenses and in the fractured near surface (van der Kamp and Hayashi, 2009). The hydraulic conductivity of soils and till decreases exponentially with depth from the order of 10 m d^{-1} at the surface to the order of 10^{-5} m d^{-1} in the tight clay rich tills below ~ 5 m (Figure 3.5) (Hayashi et al., 1998a; Bodhinayake and Si, 2004; van der Kamp and Hayashi 2009). This is conceptualized as a shallow transmission aquifer overlying an aquitard. Below the catchment a confined aquifer is present within a sandy layer at a depth of ~25 m. Hydrological interactions between the aquifer and the near surface are thought to be negligible due to the slow vertical movement of water through the till aquitard (van der Kamp and Hayashi, 2009).

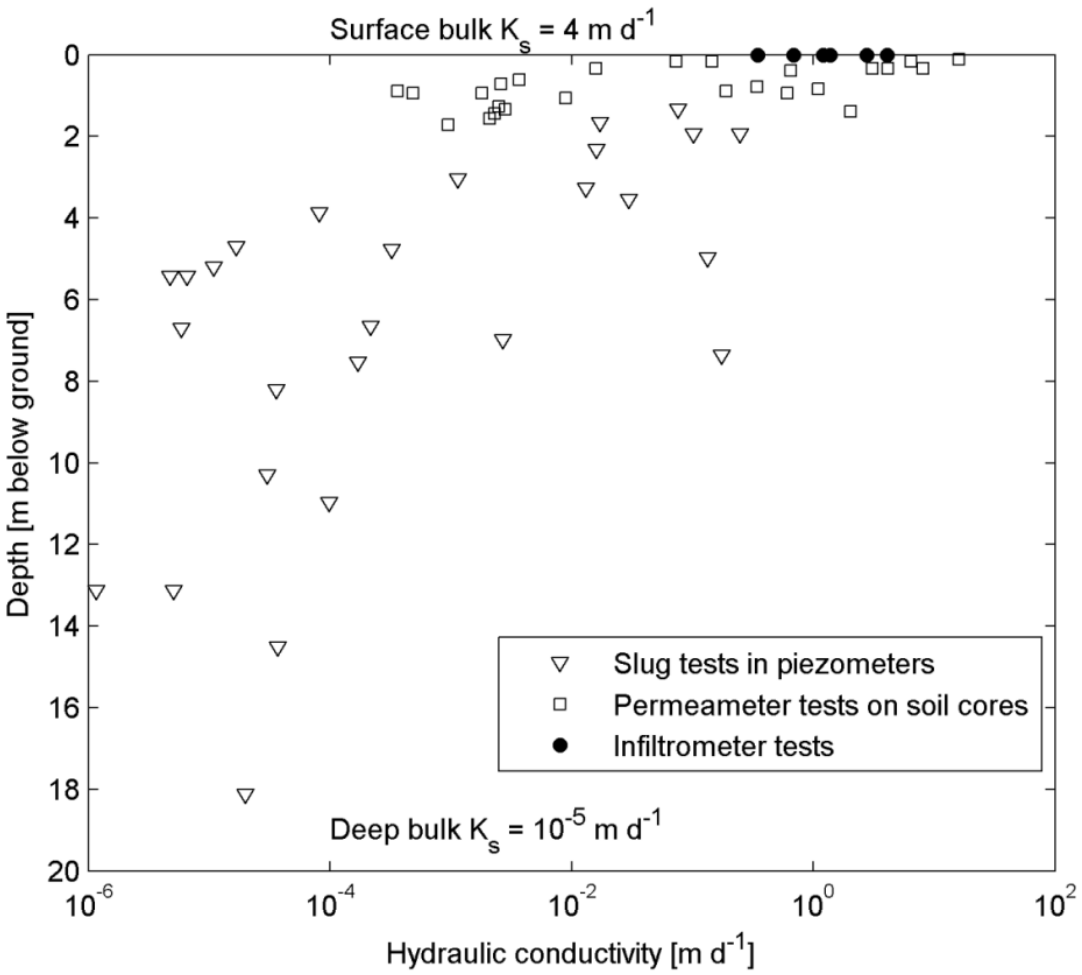

Figure 3.5: Hydraulic conductivity profile of glacial till from field measurements at SDNWA. Data source: Hayashi et al., 1998a; Parsons et al., 2004; van der Kamp et al., 2003.

CHAPTER 4 : METHODS

4.1 Pond water budget

Field work was carried out between 29 March and 9 Aug 2013 and focused on the water budget of the pond complex between the two flumes described above and comprising the four ponds connected by the intermittent St. Denis Creek. All of the components of the water budget are expressed as an equivalent pond-water depth, that is, the daily average pond volume divided by the daily average pond surface area. Pond stage was monitored at half-hour intervals using unvented Solinst Levelogger pressure transducers in each pond corrected for changes in barometric pressure using a Solinst Barologger barometer mounted near Pond 1. Pond area changed continuously during the study period, thus, observed surface storage was calculated using the daily average pond volume and area. The relationship between pond volume, $V_{p,i}$ (m^3), surface area, $A_{p,i}$ (m^2), and stage, $h_{p,i}$ (m), was determined for each pond using bathymetry and LiDAR data following the methods outlined in Hayashi and van der Kamp (2000) and Minke et al. (2010):

$$A_{P,i} = s_i(h_{p,i})^{2/p_i} \tag{4.1}$$

$$V_{p,i} = \left(\frac{s_i}{1+\frac{2}{p_i}}\right)\left(\frac{h_{p,i}^{\,1+\frac{2}{p_i}}}{1^{\frac{2}{p_i}}}\right) \tag{4.2}$$

where s_i (m^2) is a scaling constant, which is equal to the area of water surface when $h_{p,i} = 1$, and p_i (-) represents the profile of the depression.

The water budget of each pond is given by:

$$\frac{dS_i}{dt} = P_d + R + G - E + Q_i - Q_o + \xi \tag{4.3}$$

where P_d is direct precipitation, R is surface runoff into the pond, G is net groundwater exchange, E is open water evaporation, Q_i and Q_o are channelized inflow and outflow, respectively, and ξ is

the residual (all in units of mm d^{-1}). Minke et al. (2010) report volume errors of <10% using the same methods for determining pond depths and V-A-h relationships. Thus, the accuracy of the storage term is estimated as ± 10%, and the accuracy of all other components of the water budget are given below.

The total pond storage over the entire reach, S_T (mm), is given by the sum of the individual pond volumes divided by the sum of surface area of individual ponds:

$$S_T = \frac{\sum_{i=1}^{4} V_{p,i}}{\sum_{i=1}^{4} A_{p,i}} \quad (4.4)$$

4.1.1 *Direct precipitation*

Rainfall (mm d^{-1}) was measured at half-hourly intervals using a Texas Electronics TE525M tipping bucket rain gauge at a terrestrial climate station on-site (accuracy within 5%) (Figure 3.1).

4.1.2 *Runoff*

To estimate runoff, the watershed was divided into four sub-catchments corresponding to the contributing area of each pond. Each sub-catchment was further subdivided into the following land cover classes, *LCA*, based on landcover and aspect: fallow (east aspect), crop (north aspect), grass (north, west, south, and flat aspects), pond, and riparian vegetation. Each land cover class, *LCA*, has an associated area, A_{LCA}. The surface runoff term, R (mm d^{-1}), is comprised of three distinct fluxes or flows: infiltration excess snowmelt runoff, r_M (mm d^{-1}), infiltration excess rainfall runoff, r_R (mm d^{-1}), and runoff originating directly from upland ponds, r_S (m^3 d^{-1}). The diffuse runoff terms, r_M and r_R, were assumed spatially uniform over the sub-units. r_S was observed to occur periodically during the melt period, as concentrated sheet or

channelized flow at discrete spatial locations. Runoff (accuracy ± 50%) into each pond from the hillslopes is given by the sum of these three terms, aggregated over different landcover class/aspect areas and then converted to depth over the area of the pond surface, A_p (m^2), i.e.:

$$R = \frac{\sum_{LC=1}^{N} r_{R,LCA} A_{LCA} + r_{M,LCA} A_{LCA}}{A_p} + \frac{r_s}{A_p} \quad (4.5)$$

4.1.3 *Snowmelt runoff*

Snowmelt may infiltrate directly into the soil or runoff over the hillslopes into ponds. For each individual LCA, the estimated total snowmelt, M (mm d^{-1}), was combined with an estimate of infiltration capacity of the frozen soils, f (mm d^{-1}), such that melt runoff to the reach ponds is given by:

$$r_{M,LC} = \max(M_{LC} - f_{LC}, 0). \quad (4.6)$$

A stratified snow survey was completed just prior to the initiation of snowmelt following the method described by Pomeroy and Gray (1995). The snow survey consisted of eight snow courses in each of the land covers and aspects represented within the catchment. Each snow course was completed along transects with 20 sample points spaced at approximately 5 m intervals. At every fifth depth measurement a density sample was collected. Snow depth and snow density samples were taken with an Eastern Snow Conference snow sampler (accuracy ± 5%). Mean snow water equivalent, SWE (mm), was calculated for each point using:

$$SWE = \frac{\rho_s d}{\rho_w} \quad (4.7)$$

where ρ_s is the average snow density (kg m^{-3}) for each snow course, d is snow depth at the point (mm), and ρ_w is the density of water (1000 kg m^{-3}). The SWE values were averaged over each snow course to find the mean SWE for each landcover. Average catchment SWE was estimated

by taking a weighted mean by landcover fraction. To account for snowfall after the snow survey, a snowboard was installed at the upstream flume and monitored daily. Measurements of depth and density of snow on the board were used to calculate SWE using the above equation and added to the snow survey values from each of the snow courses. For comparison, the long-term average of the spring snowpack was calculated using historical snow survey data collected at SDNWA.

To quantify snowmelt, ablation lines were installed in each landcover type alongside each snow course to determine daily ablation rate, M_a (mm d^{-1}), using the method described by Heron and Woo (1978). For a given day, the depth of ablation, M_a, was given by:

$$M_a = (h_{(t-\Delta t)} - h_{(t)})/\rho_s \tag{4.8}$$

where $h_{(t-\Delta t)}$ and $h_{(t)}$ are the average heights of the snow surface above an arbitrary datum, measured manually on a daily basis. These measurements were obtained by averaging the distance of approximately ten points on the snow surface below a taut wire held in place between two steel rods frozen into the ground, at time $t - \Delta t$ and t, and ρ_s is the density of the snow during the period Δt sampled from the surface of the snowpack of the ablation line.

The daily snowmelt, M (mm d^{-1}), at each of the ablation lines was calculated as in Guan et al. (2010) using the equation:

$$M = (M_a - S_b)a_s \tag{4.9}$$

where S_b is sublimation loss (mm d^{-1}) calculated using latent heat flux data (measurement described below) and a_s (m^2) is the fraction of snow-covered area in the specific landcover/aspect of the ablation line estimated from daily visual observation. Guan et al. (2010) estimate the accuracy of this method to be ± 25%.

Sublimation losses were calculated using latent heat flux data, Q_e (W m^{-2} positive upward from the surface), from the climate station at the south end of the catchment (Figure 3.1). The eddy covariance method was used, employing 10-Hz measurements of the vertical wind speed, w (m s^{-1}), air temperature, T (°C), and water vapor density, q (g m^{-3}). Wind speed was measured using a 3-D ultrasonic anemometer (Campbell Scientific CSAT-3), while water vapor density was measured using an open-path gas analyzer (Campbell Scientific EC150 CO_2/H_20 gas analyzer) located 15 cm away and at the same height as the sonic anemometer. The statistics (means and covariances) of the high-frequency data were collected and processed at 30-min intervals using a datalogger (Campbell Scientific CR3000). Corrections to the eddy covariance measurements include 2-D coordinate rotation (Baldocchi et al., 1988), air density fluctuations (Webb et al., 1980), sonic path length, high-frequency attenuation, and sensor separation (Massman, 2000; Horst, 1997).

The infiltration capacity of each landcover class under frozen soil conditions was calculated using the method of Gray et al. (1985) for prairie regions, as used by Woo and Rowsell (1993) at SDNWA. The snowmelt infiltration capacity, f(mm) is given by:

$$f = \left(1 - \theta_p\right) SWE^{\,n} \tag{4.10}$$

where n is a parameter that Gray et al. (1985) suggest to be equal to 0.584 based on empirical observations, θ_p is the pore saturation (%), which is a ratio of fall volumetric water content averaged from a 128 point neutron probe survey along a 576 m transect with 4.5 m intervals, and soil porosity. Mean soil porosity values given in the literature for SDNWA are 0.56 in the uncultivated grassed hillslopes, 0.5 in the cultivated areas, and 0.53 surrounding the wetlands (van der Kamp et al., 2003; Parsons et al. 2004). Volumetric water content of the top 30 cm was

measured during snowmelt on the north hillslope adjacent to Pond 125 at half hour intervals using a Campbell Scientific CS615-L water content reflectometer.

4.1.4 *Rainfall runoff*

During rainfall events, hillslope runoff, r_R (mm d^{-1}) was calculated for each landcover class as the residual of rainfall rate, w (mm d^{-1}) and infiltration capacity, f^*(mm d^{-1}):

$$r_{R,LC} = \max(w - f^*_{LC}, 0). \tag{4.11}$$

4.1.5 *Surface runoff from upland ponds*

During snowmelt and after rainfall events the catchment was surveyed to determine which upland ponds were contributing overland flow, r_S (m^3 d^{-1}), to the reach. Where possible, this flow rate was gauged directly by measuring the cross sectional area of flow and the average velocity using a floating disc.

4.1.6 *Evaporation*

Actual evaporation from open water surfaces, E (mm d^{-1}), was calculated using the Combination Model (Oke, 1987):

$$E = \frac{1}{\lambda}\left(\frac{\Delta(Q^* - J_w) + \frac{\rho_a c_p D}{r_a}}{\Delta + \gamma}\right) \tag{4.12}$$

where λ is the latent heat of vapourization (MJ kg^{-1}), Δ is the slope of the saturation vapour pressure temperature relationship (kPa °C^{-1}), Q^* is the net radiation (MJ m^{-2} d^{-1}), J_w is the change in heat storage (MJ m^{-2} d^{-1}), ρ_a is the air density (kg m^{-3}), c_p is specific heat of air (0.001013 MJ kg^{-1} °C^{-1}), D is the vapour pressure deficit (kPa), r_a is aerodynamic resistance (d m^{-1}), and γ is the

psychometric constant (kPa °C^{-1}). Meteorological measurements were made from a raft installed on Pond 1 (Figure 3.1). The station measured air temperature, T_a (°C), relative humidity, RH (%), wind speed, u (m s^{-1}), wind direction, u_{dir} (degree), net radiation, and surface water temperature, T_s (°C). Sensors were connected to a Campbell Scientific CR1000 datalogger. Data were scanned every 10 seconds and averaged at half-hour intervals. A HOBO thermistor string was installed adjacent to the raft to measure the depth profile of water temperature.

The change in heat storage, J_w (MJ m^{-2} d^{-1}), was determined following the method of Blanken et al. (2000). A thermistor string was attached to a cable anchored to the pond bottom from the floating meteorological station; HOBO thermistors were located every 25 cm to a depth of 1.25 m. Temperature measurements were taken every 30 minutes and averaged over each day. The mean water temperature $\overline{T_W}$ (°C) was given by:

$$\overline{T_W} = \frac{1}{z}\sum_{i=1}^{n} T_{wi}\Delta z \tag{4.13}$$

which allows the calculation of J_w as:

$$J_w = \rho c_p \frac{\Delta \overline{T_w}}{\Delta t} z \tag{4.14}$$

where z is depth (m), T_{wi} is the water temperature (°C) at the individual thermistor, Δz is the depth segment assigned to that thermistor, ρ is the density of water (kg m^{-3}), cp is the specific heat of water (J °C kg^{-1}), and t is time (s). Spence et al. (2003) reported an accuracy of ± 20% using similar methods.

4.1.7 *Streamflow*

Stream stage in Parshall flumes and V-notch weirs at the inlet and outlet of the study catchment was monitored continuously at 30-minute intervals using Solinst Leveloggers. Stream

discharge through the flumes was calculated using a stage-discharge equation derived for the geometry of the flumes (ISO, 1992):

$$Q = 1.403h^{1.548} \quad (4.15)$$

where Q is discharge ($m^3\ s^{-1}$), and h is upstream stage at the flume entrance section (m). The range of heads where this equation remains accurate is 0.05 – 0.75 m, thus during low flows the V-notch weir was used to determine flow rate (accuracy within 5%). Flow rate was converted to a flux, Q_i and Q_o (mm d^{-1}), by dividing by the pond area, A_p (m^2).

4.2 Groundwater

A transect of piezometers extended from the southern to the northern hillslope across Pond 125 (Figure 3.1). The northern piezometers were located 5 m, 10 m, 40 m, and 80 m from the pond at depths of 1.64 m, 3.06 m, 3.8 m, and 5.5 m, respectively. Piezometers were constructed from 5.08 cm inside diameter PVC tubing installed in 10.16 cm diameter boreholes drilled with a Giddings rig. Screens were 60 cm in length, slotted every 0.64 cm and capped at the bottom. Sand packs were installed around screens and were sealed to the surface with bentonite pellets. The piezometers on the southern hillslope were located 2 m and 44 m from Pond 125 at depths of 2.9 m and 3.75 m, respectively, and constructed of 3.2 cm inside diameter PVC tubing. Piezometers were monitored at half hourly intervals using Solinst Leveloggers and calibrated with manual measurements taken every month. Fluctuations in barometric pressure were corrected using readings from a Solinst Barologger located at the raft.

Hydraulic heads were calculated at each piezometer relative to mean sea level to determine the horizontal hydraulic gradient, which was used to infer temporal variations in groundwater exchange between the pond and riparian area or upland. Due to the inherent

uncertainty in scaling up from the point scale to the landscape scale, net groundwater exchange between ponds and uplands was estimated using the water budget approach, where Equation 4.3 was rearranged and ξ was assumed to be zero to solve for net groundwater exchange, G (m^3 d^{-1}). It is recognized that the groundwater term, G, will also include the propagation of errors from each of the measured water budget terms.

To discern where groundwater-surface water connectivity may have occurred in the catchment, the water table depth in the catchment was interpolated using the kriging tool in Surfer 9 (Golden Software, Golden, CO, USA). Piezometer and pond level data from Pond 125 and the five smaller ponds surrounding Pond 125 were used to map the water table elevation. The water table elevation was then subtracted from the DEM to give water table depth below ground surface. The LiDAR DEM of this site had an elevation bias of 0.03 m and a RMSE of 0.14 m, as calculated by Toyra et al. (2006).

4.3 Streamflow response

To examine how the groundwater input into ponds affects downstream streamflow response, we compared the actual streamflow hydrograph with a modelled hydrograph assuming no net groundwater exchange. A power-law relationship between total reach surface storage, S [mm], and streamflow, Q_O [m^3 d^{-1}], was assumed:

$$Q_{O\,(t)} = aS_{(t)}{}^{b} \tag{4.16}$$

where a and b are parameters that were identified by fitting a curve to the relationship between Q_O and S for each runoff event. This calibrated relationship was then applied to calculate the average daily simulated streamflow, Q_S, with groundwater inputs assumed to be zero. Qs is a

function of a modified storage term in which the groundwater exchange term is removed. The modified storage term is given by:

$$S_{(t+1)} = S_{(t)} + P_{d_{(t)}} + R_{(t)} - E_{(t)} + Q_{i_{(t)}} - Q_{S_{(t)}} \quad (4.17)$$

Hence, Q_S is given by:

$$Q_{S_{(t+1)}} = aS_{(t+1)}{}^{b} \quad (4.18)$$

and subsequently through time $t + 2, \ldots, t + n$.

Runoff ratios were calculated for the observed and simulated hydrographs. Event streamflow, Q_e, was estimated by separating hydrographs using the recession curve equation from Dingman (1973):

$$Q_t = Q_o e^{\left(\frac{-t}{t^*}\right)} \quad (4.19)$$

where Q_o is the discharge on the day immediately prior to the runoff event, and Q_t is the calculated streamflow on day t, assuming that the event did not occur. The recession coefficient, t^* (days), was taken as the reciprocal of the slope of the best fit line from regression between ln(Q) and t for the falling of the hydrograph prior to the event. Event runoff was calculated as the sum of the daily difference of Q_t and observed Q until Q_t exceeded Q. The runoff (m^3) was converted to depth by dividing by the area of the entire watershed (10.3 km^2). Runoff ratios (Q/P) were calculated for all snowmelt and rainfall events.

4.4 Model development

4.4.1 *Model structure*

Simple hydrological models may be useful for improving understanding of the complexity of prairie pothole hydrology under changing conditions. Measured pond levels, groundwater levels, and discharge can be used to validate the performance of these models

(Krasnostein and Oldham, 2004), which may provide useful information for exploring parameter identifiability and equifinality, and for elucidating processes that dictate the dynamics of basin storage and streamflow. The modelling experiment design explored mainly the effects of a range of different infiltration capacities, contributing areas, and subsurface transmission parameters, as field methods described above for estimating these parameters were highly uncertain. A conceptual modelling approach was used to supplement the field study, which was aimed at determining if subsurface flow was important for maintaining pond storage and streamflow. The goal of the modelling experiment was not to develop a tool for management purposes, but to perform a qualitative thought experiment, which tested a conceptual model of physical processes.

The model structure consisted of a series of three stores representing unsaturated soil, saturated soil, and pond storage (Figure 4.1). The model structure was comprised of four units, for each one of the four reach ponds, that each contained all three stores (pond, saturated hillslope areas and unsaturated hillslope areas). The saturated and unsaturated hillslope stores were lumped into an upland store that represented the contributing area to each pond. This contributing area included hillslopes directly adjacent to the major ponds, as well as multiple upland ponds and their individual contributing areas. The volume in each store was calculated on a daily time step. The fluxes out of and into the drainage basin, consisting of four units of wetland and upland, were via the atmosphere, inflow into the first pond, and discharge from the last pond. The model was coded and run in MATLAB.

The model structure was based on the conceptual understanding of prairie hydrology discussed in Chapter 2. The pond storage, h_p, receives flow from the saturated store, G, direct precipitation, P, and inflow, I. The unsaturated soil storage, S_s, receives snowmelt, M, and rainfall, P, which are partitioned into snowmelt and rainfall infiltration, M_i and P_i, with the

remainder directed to surface runoff, *R*. Pond storage loses water through evaporation, *E*, and outflow, *O*. The soil storage loses water through drainage, *D*, to the saturated store when soil storage exceeds the threshold of field capacity, *FC*. The groundwater store, h_g, receives water through drainage from the soil store and loses water (or gains water, depending on the gradient), to pond storage.

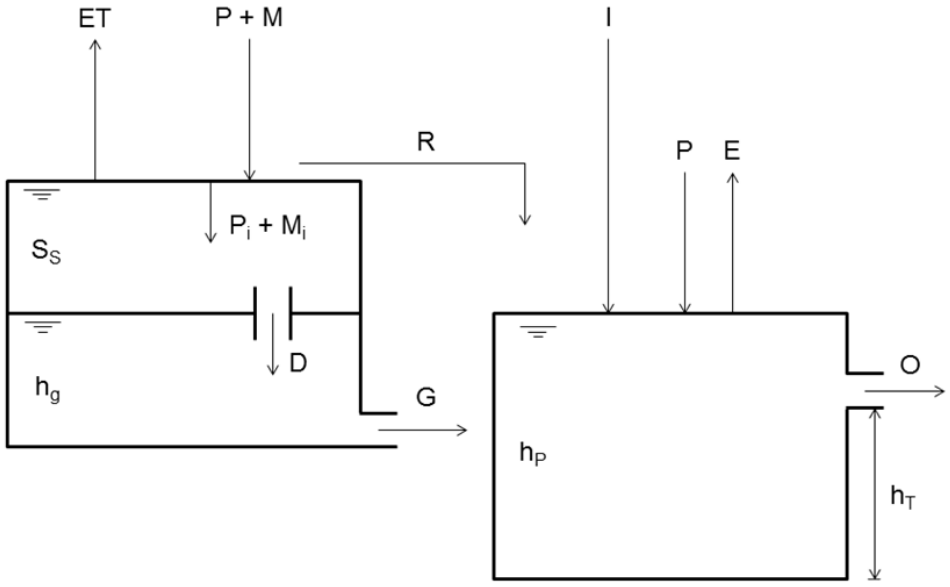

I	inflow	**h_P**	pond store	**P_i+M_i**	infiltration
P	precipitation	**h_g**	groundwater store	**R**	overland flow
M	snowmelt			**D**	recharge to groundwater
E	evaporation	**S_s**	soil moisture store	**O**	outflow
ET	transpiration	**h_T**	pond storage threshold	**G**	groundwater exchange

Figure 4.1: Model structure.

4.4.2 *Driving data*

Driving data used for the model simulations were field data collected during the 2013 field season. These data include: inflow, I (m^3 d^{-1}), collected at the upstream flume; direct precipitation, P (m d^{-1}), collected at the terrestrial climate tower; an average snowmelt rate, M (m d^{-1}), estimated from pro-rating the area represented by each of the eight ablation lines; pond

evaporation, E (m d^{-1}), calculated using the method described in section 4.1.6; and actual evapotranspiration, ET (m d^{-1}), which was calculated using latent heat flux data from the eddy covariance sensors on the terrestrial climate tower.

The model requires initial conditions for each of the stores. The initial pond level (h_{p0}) was observed. Initial groundwater level (h_{g0}) was set to the same value as the pond storage, so there was no gradient between the hillslope and pond for the first time step. Field capacity was set to the same arbitrary value for all the model runs, and the initial soil moisture storage (S_{s0}) was calibrated such that it represented a soil moisture deficit below saturation.

4.4.3 *Quantitative representation of catchment*

Flux equations:

Snowmelt runoff, R_S (m d^{-1}), is given by the equation:

$$R_S = M \propto_M \tag{4.20}$$

where M is snowmelt (m d^{-1}), and alpha, α_M (-), is a ratio for partitioning snowmelt into runoff and infiltration. Thus, snowmelt infiltration, M_i (m d^{-1}), is given by:

$$M_i = M(1 - \propto_M). \tag{4.21}$$

The rainfall infiltration, P_i (m d^{-1}), is given by the equation:

$$P_i = P(1 - \propto_R) \tag{4.22}$$

and rainfall runoff, R_R (m d^{-1}), is given by:

$$R_R = P \propto_R \tag{4.23}$$

where P is rainfall (m d^{-1}) and alpha, α_R (-), is a ratio for partitioning rainfall into runoff and infiltration. Soil drainage, D (m d^{-1}), to the groundwater store is given by the equation:

$$D = \max(0, S_s - FC) \tag{4.24}$$

where S_s is the depth of soil water stored (m), FC is the field capacity of the soil (m), and max indicates the greater of the two values 0 and $S_s - FC$.

Flow equations:

Exchange between the groundwater and pond store, G (m^3 d^{-1}) is governed by the equation:

$$G = T\,W\left(h_g - h_p\right)/L \tag{4.25}$$

where $\left(h_g - h_p\right)$ is the difference in head between the groundwater store, h_g, and the pond store, h_p (m), W is pond circumference (m), and T and L are parameters representing transmissivity (m^2 d^{-1}) and hillslope length (m), respectively. Surface outflow from each pond, O (m^3 d^{-1}) is calculated using the equation:

$$O = a\left(h_p - h_T\right)^b \tag{4.26}$$

where h_T is the pond spill threshold (m), and a (m^2 d^{-1}) and b are coefficients that determine the power law relationship between discharge and pond level.

Governing equations:

The equations governing the change in volume in each of the stores are:

$$\frac{dSs}{dt}A_{hf} = Pi\,A_{hv} + Mi\,A_{hv} - T\,A_{hv} - DA_{hf} \tag{4.27}$$

$$\frac{dhg}{dt}S_yA_{hf} = D\,A_{hf} - G \tag{4.28}$$

$$\frac{dhp}{dt}\frac{dV}{dhp} = PA_{pv} - EA_{pv} + R_RA_{hv} + R_MA_{hv} + G + I - O \tag{4.29}$$

$$\frac{dV}{dhp} = \frac{s}{(1+\frac{2}{p})(1^{\frac{2}{p}})}(1 + 2/p)\left(h_{pv}^{2/p}\right) \tag{4.30}$$

where S_y is the specific yield (-).

A_{hf} is the fixed (initial) area of the hillslope (m^2):

$$A_{hf} = \pi\left({r_{hf}}^2 - {r_{pf}}^2\right) \tag{4.31}$$

A_{hv} is the variable area of the hillslope (m^2):

$$A_{hv} = \pi({r_{hf}}^2 - {r_{pv}}^2) \tag{4.32}$$

and A_{pv} is the variable area of the pond surface (m^2) (Figure 4.2):

$$A_{pv} = \pi\, {r_{pv}}^2 \tag{4.33}$$

where r_{hf} is the fixed radius of the hillslope and pond, r_{pf} is the initial radius of the pond, and r_{pv} is the dynamic pond radius.

Water level (h_p) in the pond is related to pond volume, V, and pond area, A_p, by volume-area-depth relationships from Hayashi and van der Kamp (2000):

$$A_P = s(h_p)^{2/p} \tag{4.34}$$

$$V = \left(\frac{s}{1+\frac{2}{p}}\right)\left(\frac{{h_p}^{1+\frac{2}{p}}}{1^{\frac{2}{p}}}\right) \tag{4.35}$$

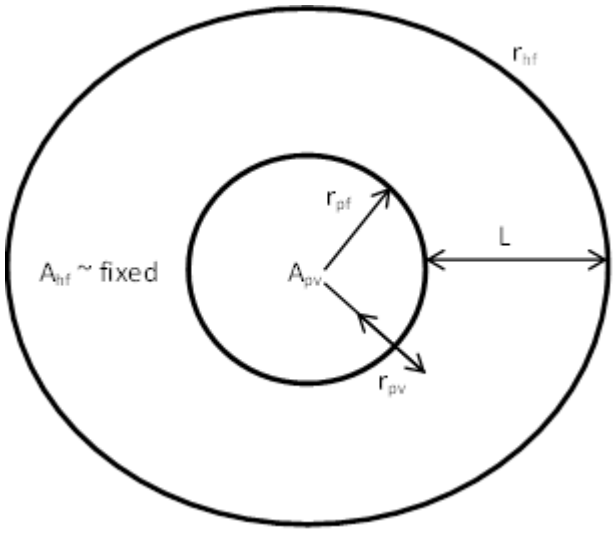

Figure 4.2: Modelled pond and hillslope areas.

4.4.4 *Parameter identification*

Measured parameters included the shape coefficient, s (m^2), and profile coefficient, p (-), used for calculating the volume and area of the ponds, and the pond threshold height, h_T (m), which was taken as the maximum pond stage evaluated from the LiDAR DEM in ArcGIS 10.1. Parameters requiring optimization were α_M, α_S, T, S_y, L, a, and b, and the initial soil moisture storage, S_{s0}. To reduce the number of free parameters to be optimized the same α_M, α_S, T, S_y, and S_{s0} values were used for each of the four hillslope-pond units. Hillslope length, L, and pond drainage coefficients, a and b, were necessarily different for each unit. We used a GLUE approach to explore the multivariate parameter space. The calibration strategy was a simple Monte Carlo simulation, where a number of realizations were generated by randomly selecting parameter values from a specified uniform random range. Monte Carlo simulations are widely used to determine the impacts of model and parameter uncertainty on simulation results. The GLUE approach recognises that the model output could result from a variety of combinations of parameters, rather than a single combination (Beven, 2012). Thus, in this experiment all parameter distrubtions were considered together, i.e., no parameters were held fixed except those that were measured. Model outputs were generated for each of 100,000 realizations. An objective function, RMSE, was used to judge each model realization against observed discharge. For every parameter, plots of each parameter value against objective function were created. Realizations that had an RMSE value below a specified threshold were considered "behavioural".

The parameter ranges were selected based on a-priori understanding. The runoff-partitioning parameters, α_M and α_R, were sampled from a random distribution between 0 and 100% (Table 4.1). Although there was no observed rainfall runoff on hillslopes adjacent to the

reach ponds during the study period, the model needed to be able to account for surface runoff from snowmelt and rainfall because the hillslope bucket represents the contributing area of each pond, where surface runoff from upland ponds was observed. The range of initial soil moisture storage sampled was 0 m (relative field capacity) to - 0.1 m. The range of hillslope lengths for each pond, $L_1 – L_4$, was calculated assuming a circular catchment from the area of adjacent hillslopes, to the gross contributing area for each pond. The ranges of hillslope length were determined using areas derived from the catchment DEM in ArcGIS.

Table 4.1: Model parameters and sample ranges.

Parameter	**Type**	**Description**	**Sample range**
α_R and α_M (-)	Free	Runoff partitioning ratio	0 – 1
a (m^2 d^{-1})	Free	Pond drainage constant	10000 - 1000000
b (-)	Free	Pond drainage exponent	1 – 4
T (m^2 d^{-1})	Free	Transmissivity	50 - 500
S_y (-)	Free	Specific yield	0.005 – 0.2
S_{s0} (m)	Free	Initial soil moisture deficit	0 – -0.1
L_1 (m)	Free	Hillslope length	288 – 366
L_2 (m)	Free	Hillslope length	195 – 271
L_3 (m)	Free	Hillslope length	82 – 82
L_4 (m)	Free	Hillslope length	167 – 349
w (m)	Observed	Pond circumference	1012; 703; 221; 486
h_T (m)	Observed	Pond spill threshold	3.11; 3.33; 1.27; 2.18
s (m^2)	Observed	Pond shape coefficient	21570; 8155.4; 3205; 8575.2
p (-)	Observed	Pond profile coefficient	1.67; 1.51; 1.89; 2.01
FC	Fixed	Field capacity	0

CHAPTER 5 : REACH WATER BUDGET AND HYDROLOGICAL PROCESSES

This chapter describes the pond water budget and groundwater behaviour observed at the study site. These observations are used to infer the relative importance of surface and subsurface fluxes to runoff response in the catchment.

5.1 Pond water budget

5.1.1 *Rainfall*

Rainfall measured at the climate tower was considered to be uniform over the ~ 1 km^2 catchment. Individual events ranged from 0.1 mm d^{-1} to 37.6 mm d^{-1}, with a total of 178 mm falling over the period 10 May – 9 August (Figure 5.1). The monthly rainfall for May, June, and July was 20.3 mm, 105.3 mm, and 49.7 mm, respectively. For comparison, the 30-year climate normal values (1978-2007) for the Environment Canada Saskatoon Airport station 50 km to the west are 48 mm, 67 mm, and 59 mm for the same months, indicating that June was an abnormally wet month (157% of normal), and May and July were drier than average (42% and 85% of normal, respectively).

5.1.2 *Evaporation*

Total pond evaporation for the period 10 May – 9 August was 228 mm, and averaged 2.5 mm d^{-1} (Figure 5.2). For comparison, Woo and Rowsell (1993) calculated 186 mm, 213 mm, and 206 mm of evaporation from a pond in SDNWA during the summer season (approximately the end of March to mid-August) from 1989 – 1991. The average evaporation rates in May, June, July and August were 1.1 mm d^{-1}, 2.0 mm d^{-1}, 3.5 mm d^{-1} and 2.4 mm d^{-1}, respectively.

Evaporation exceeded precipitation in May, July, and August. In June precipitation exceeded evaporation by 44 mm.

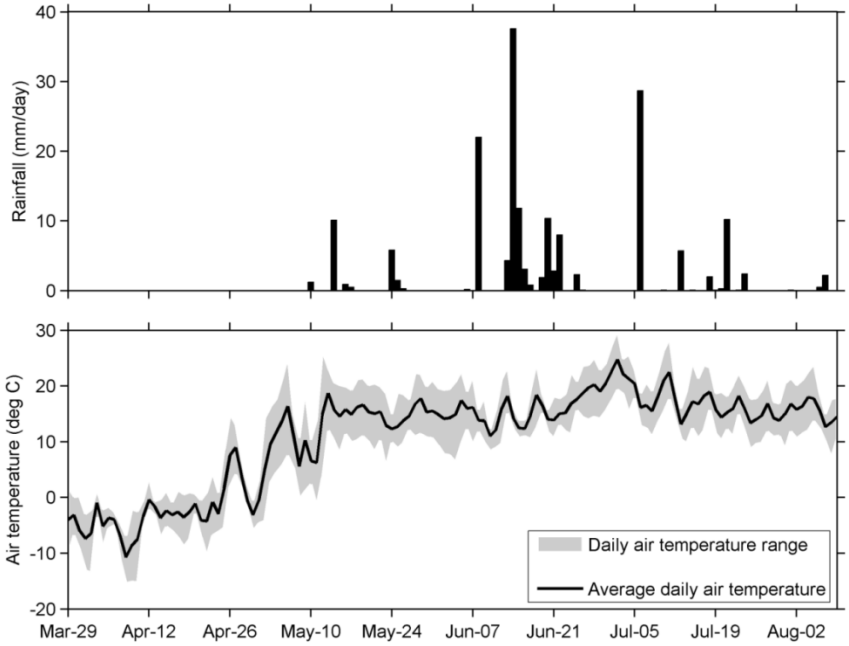

Figure 5.1: Mean daily air temperature (range is shown in grey) and total daily precipitation measured at flux tower from 29 March – 9 Aug, 2013.

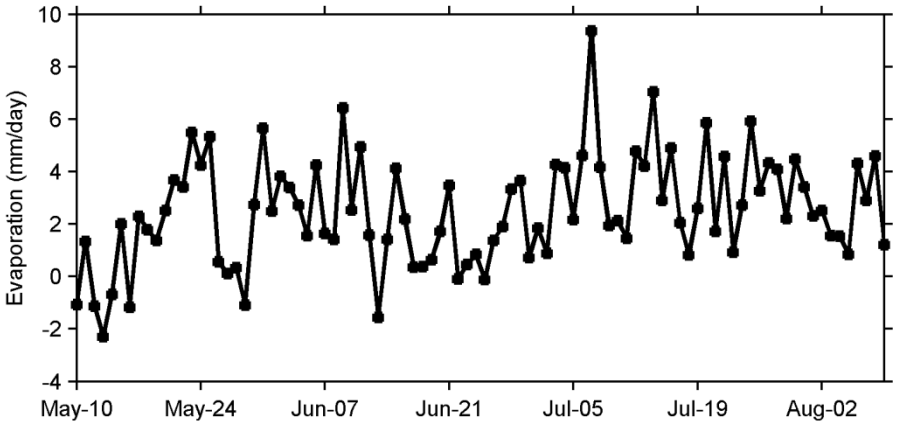

Figure 5.2: Daily open water evaporation over the period 10 May – 9 Aug, 2013.

5.1.3 *Melt*

The average spring snowpack in 2013 over the whole of SDNWA was the largest in the preceding 24 year period (Figure 5.3). Spatially averaged SWE over the study catchment at the

time of the snow survey was 94 mm, with an additional 21 mm falling over the period 29 March – 29 Apr. Sublimation accounted for 10 mm of ablation over the snowmelt period (Figure 5.4). For the period 29 March – 24 April mean daily air temperatures were below 0 °C, and thus melt rates were low (1.4 mm d^{-1} on average, Figure 5.4). As mean daily air temperatures reached 0°C the greatest daily snowmelt rates occurred on 25 and 26 April at 25 mm d^{-1} and 27 mm d^{-1}, respectively. Snow cover was largely depleted by 29 April, with the exception of trees and riparian vegetation cover, which had some snow cover until 17 May.

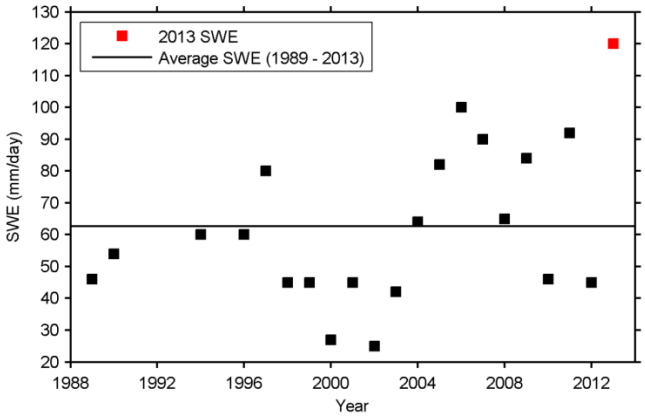

Figure 5.3: Average and yearly SWE values for SDNWA, 1994-2013.

Snow depth, snow water equivalent, and snowmelt rates varied between each land cover type and aspect (Figure 5.5). Snow cover was depleted in a sequence of fallow first, then stubble, grass, trees, and finally riparian vegetation. The greatest snow accumulation was found in trees and riparian zones: 184 mm and 457 mm, respectively, due to wind redistribution from open sites to sheltered and vegetated sites. However, these landcovers represented relatively small areas of the catchment, so their contribution to the catchment water budget was much lower, and also was delayed until after the peak streamflow. Ice on the ponds had completely melted by 10 May.

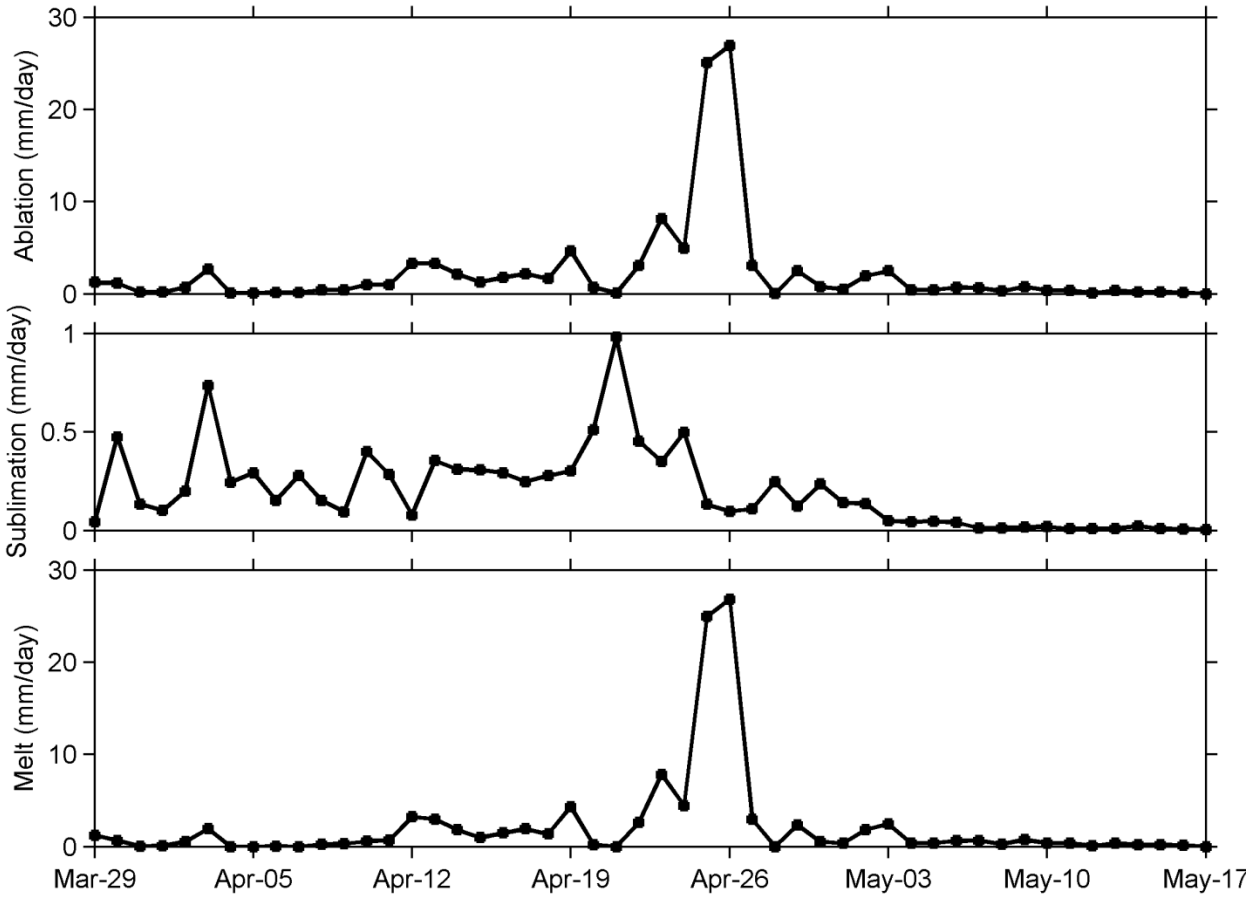

Figure 5.4: Spring of 2013 snow ablation (a), sublimation (b) and snowmelt (c) for the study catchment.

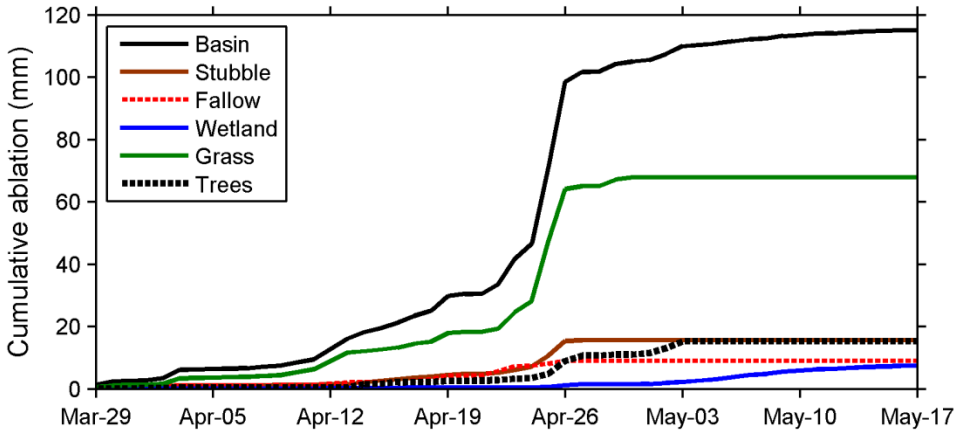

Figure 5.5: Cumulative ablation by land cover class and total basin ablation weighted by areal fraction in the study catchment from 29 March – 17 May, 2013.

5.1.4 *Runoff*

A mean volumetric water content value of 0.24 was calculated from the neutron probe survey undertaken on 17 September 2012 (Hu, unpublished data). This was used to estimate the seasonal frozen soil infiltration capacity across land cover types in the basin using Equation 4.10, which ranged from 29 mm – 100 mm (Table 5.1). Snowmelt runoff, r_M, from hillslopes began on 19 April (Figure 5.6). Snowmelt runoff rates remained at approximately 1 mm d^{-1} between 22 April – 24 April, then rose to 20 mm d^{-1} on 25 April and peaked at 26 mm d^{-1} on 26 April, two days before peak streamflow occurred at the upstream flume and four days before peak streamflow at the lower flume. After 27 April catchment snowmelt runoff was minimal as the snowpack was mostly depleted. The soil moisture content of the top 30 cm measured with the TDR probe began to rise on 26 April, indicating that the soil was thawing (Figure 5.6). Soil moisture data from the melt period indicate that the top 30 cm of soil was mainly thawed by 29 April.

Table 5.1: Total SWE and infiltration capacity of different landcover types and aspects.

Ablation Line	AL1	AL2	AL3	AL5	AL 6	AL 7	Pond 125 bluff	Pond 127
Landcover	Fallow	Crop	Grass	Grass (hayed)	Grass	Grass (hayed)	Wetland vegetation	Trees
SWE (mm)	119.3	62.9	78.1	87.9	94.9	53.3	457.5	184.8
Infiltration Capacity (mm)	47.3	32.4	49.8	40.3	44.1	29.2	100.2	60.7

No surface runoff from the hillslopes was observed during the summer rainfall events and was assumed to be zero given that the highest rainfall rate during the season was 10 mm hr^{-1} and much lower than non-frozen infiltration rates of 30 – 100 mm hr^{-1} in cultivated areas and 100 – 1500 mm hr^{-1} in grass measured by van der Kamp et al. (2003).

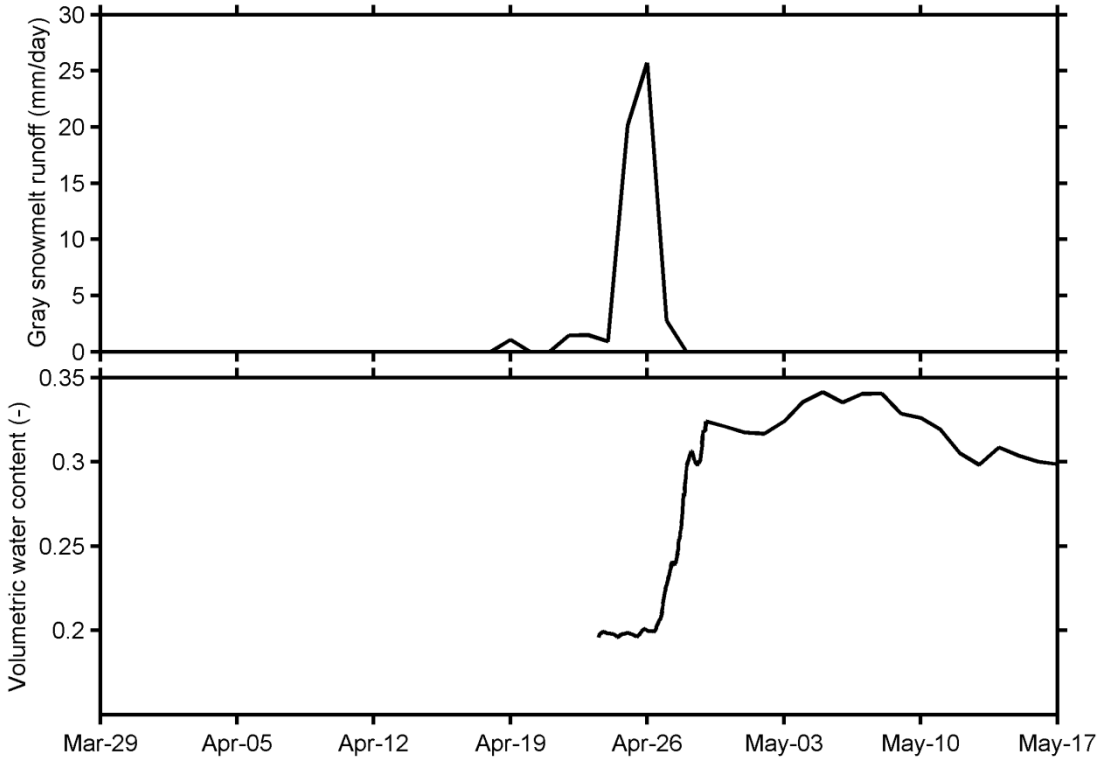

Figure 5.6: Daily hillslope runoff, r_M , and soil moisture during the snowmelt period, 29 March – 17 May, 2013.

Surface runoff contributed to the reach via a number of small upland ponds beginning 2 May (Figure 5.7). Surface runoff from upland ponds peaked on 6 May, which continued spilling until 21 May, at which time all pond levels had fallen below pond sill elevations. Runoff from upland ponds began again from 14 June – 27 June, peaking on 16 June, following 72.7 mm of rain between 13 June and 21 June. A 28.7 mm event on 6 July produced surface runoff from Pond 139 over 6 July - 8 July.

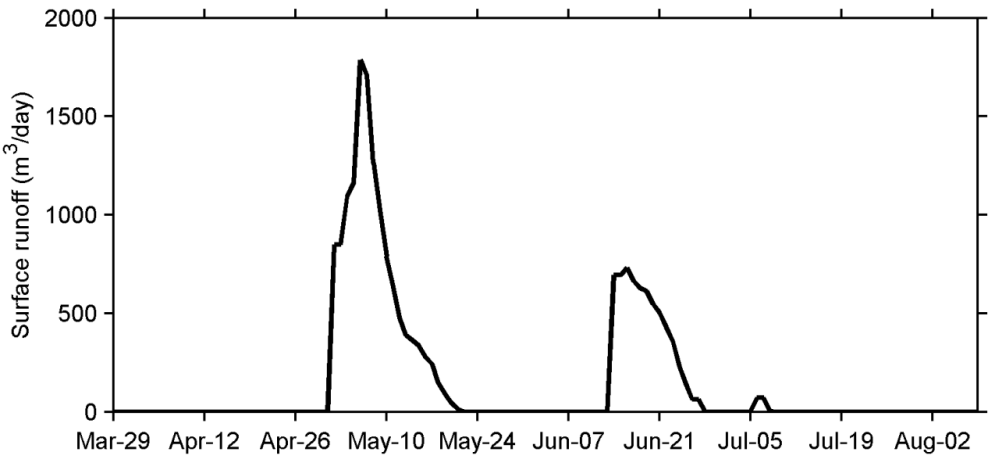

Figure 5.7: Contribution of surface runoff from upland ponds, r_S, over the period 29 March – 9 Aug, 2013.

5.1.5 *Streamflow*

Streamflow at the upstream flume began the day after peak melt on 27 April (Figure 5.8). Streamflow rose sharply to a peak discharge of 0.586 $m^3 s^{-1}$ on 28 April. Flow then receded on 29 April as the air temperature dropped below zero and the basin received another 5 mm of snowfall. Flow peaked again on 1 May and then began to recede gradually while responding to small rainfall events. Streamflow ceased above Pond 1 on 4 June. A 22 mm rain event on 8 June reinitiated streamflow. Streamflow rose to a peak of 0.154 $m^3 s^{-1}$ on 16 June following 57.6 mm of rain that fell between 13 – 16 June. Another 23.1 mm of rain was added to the catchment between 19 – 22 June increasing flow to 0.104 $m^3 s^{-1}$ by 23 June. Streamflow then receded gradually, interrupted by a 28.7 mm event on 7 July producing a small peak of 0.031 $m^3 s^{-1}$ on 8 July. Streamflow ceased on 16 July at the upstream flume for the season, except for a very small streamflow response (< 0.001 $m^3 s^{-1}$) between 24-26 July.

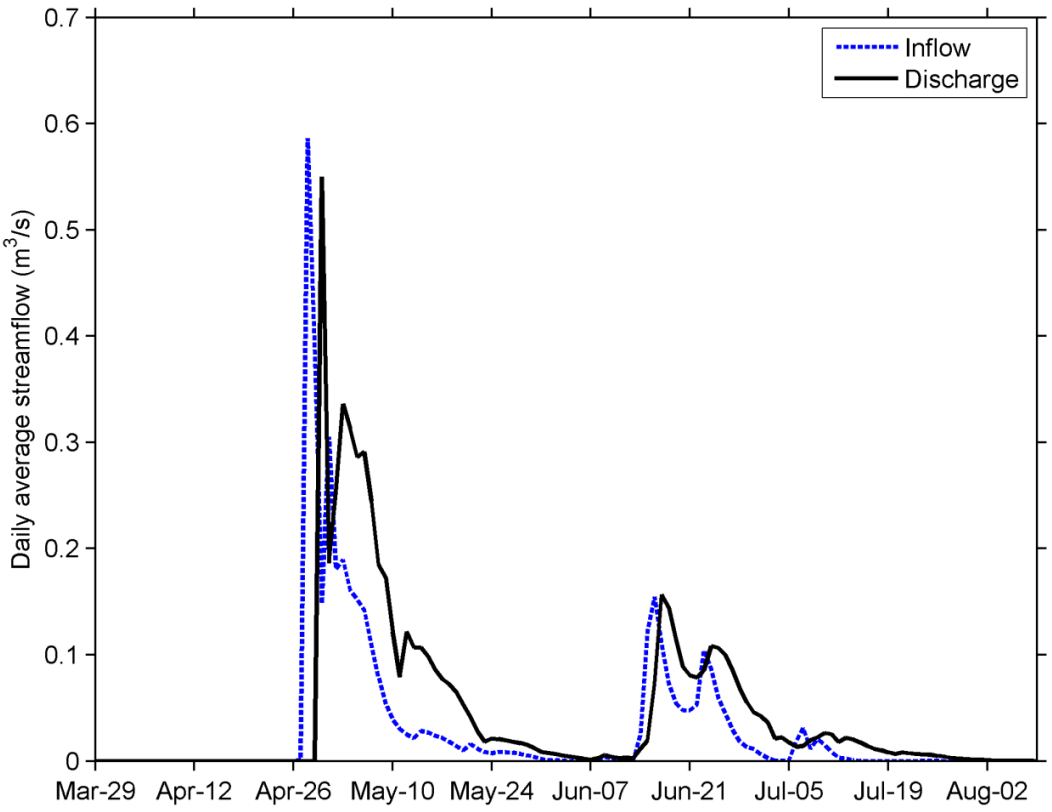

Figure 5.8: Average daily streamflow measured at the reach inlet (blue) and outlet (black) in 2013.

At the downstream flume flow was observed to be continuous over the period 30 April – 9 August. Peak spring streamflow lagged two days behind the peak at the upstream flume. A large snow dam at the outlet was breached at 10:00 am on 30 April, resulting in a peak flow of 1.90 $m^3 s^{-1}$, which receded very quickly as the pond above the outlet drained. Average discharge on 30 April was 0.550 $m^3 s^{-1}$. Streamflow at the outlet generally receded more gradually than flow at the upstream flume. Another peak in streamflow occurred mid-June, similar in magnitude to the upstream flume, 0.156 $m^3 s^{-1}$ versus 0.154 $m^3 s^{-1}$, one day after peak flow upstream (17 June). A second peak occurred on 24 June, which again lagged one day behind upstream flows. Streamflow continued to recede until the end of the season, interrupted by the 7 July rainfall

event, which produced a peak of 0.026 $m^3 s^{-1}$ on 10 July, a 5.7 mm event on 13 July (0.003 $m^3 s^{-1}$), and a 10.2 mm event on 21 July (0.001 $m^3 s^{-1}$). Streamflow ceased completely on 9 August.

5.1.6 *Storage change*

Table 5.2 shows the s and p parameters for determining V-A-h relationships derived using the methods of Hayashi and van der Kamp (2000) from LiDAR and bathymetry data. Reach storage increased substantially during the snowmelt period and reached a peak on 30 April at 265 dam^3 (Figure 5.9). Storage then decreased until 7 June and reached a second peak on 17 June. Over the study period the reach had a storage gain of 44 mm.

Table 5.2: Size and profile parameters for estimating volume of reach ponds based on pond stage.

	Pond 1	**Pond 125**	**Pond 124**	**Pond 98**
Size parameter, s (m)	21570	8155.4	3205	8575.2
Profile parameter, p (-)	1.67	1.51	1.89	2.01

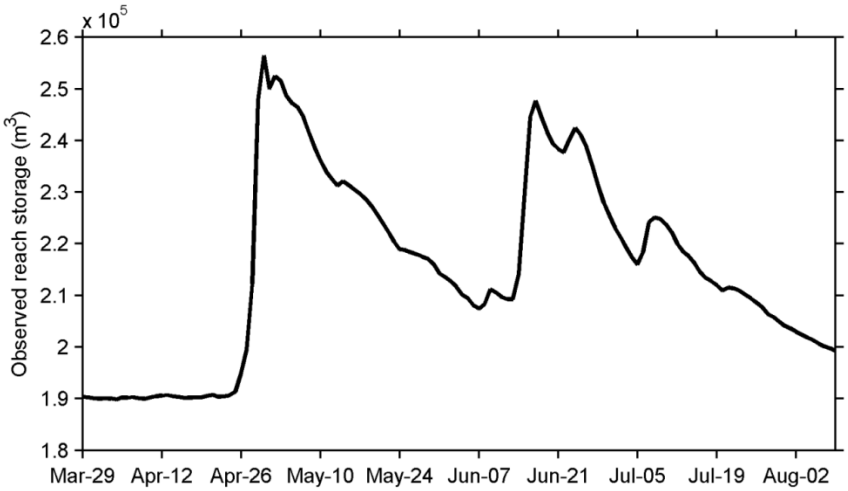

Figure 5.9: Total surface storage, S_T, in the four reach ponds over the period 29 March – 9 Aug, 2013.

5.1.7 *Water budget*

The only term in the water budget (Equation 4.3) that was not measured was the net groundwater exchange, G, as it was not possible to use direct measurements to quantify groundwater exchange over the entire reach. Figure 5.10 shows the cumulative change in storage (observed) against the cumulative net fluxes into/out of the pond complex (assuming a groundwater exchange of zero). The cumulative water budget terms are also given in Table 5.3. Vertical fluxes of direct precipitation and evaporation were the smallest components of the water budget of these large ponds, making up approximately 14% and 18% of inputs and outputs, respectively. Local surface runoff accounted for approximately 21% of total inputs to the reach. The residual (the difference between the lines in Figure 5.10, and given as a total in Table 5.3) could be due to both errors in measurements and the groundwater exchange term. Allowing for a conservatively large estimate of the errors bounds, as shown in Table 5.3, there is still a large (369 – 1295 mm) residual term, which suggests that there must have been a significant groundwater inflow into the reach ponds.

Table 5.3: Cumulative water budget for spring and summer 2013. Total inputs are precipitation and runoff. Total outputs are evaporation and net streamflow. The residual is the difference between the observed change in storage (a positive value is an increase in storage) and calculated change in storage (difference between observed inputs and outputs), and includes net groundwater exchange and water budget errors. Units are in mm. A conservative error bound is given for the water budget terms for the entire period.

	Precip. P	Evap. E	Runoff R	Streamflow In Qi	Streamflow Out Qo	Streamflow Net Qn	Chg. Stor. dS	Inputs-outputs $(\underline{P}+R+Q_i) - (E+Q_o)$	Residual
Spring	20	55	226	1513	2142	629	104	-438	542
Summer	158	173	40	633	1015	382	-60	-357	297
All	178	228	266	2146	3157	1011	44	-795	839
Error (All)	169 – 189	182 – 274	133 – 399	2039 – 2253	2998 – 3314	745 – 1275	28 – 48		369 – 1295

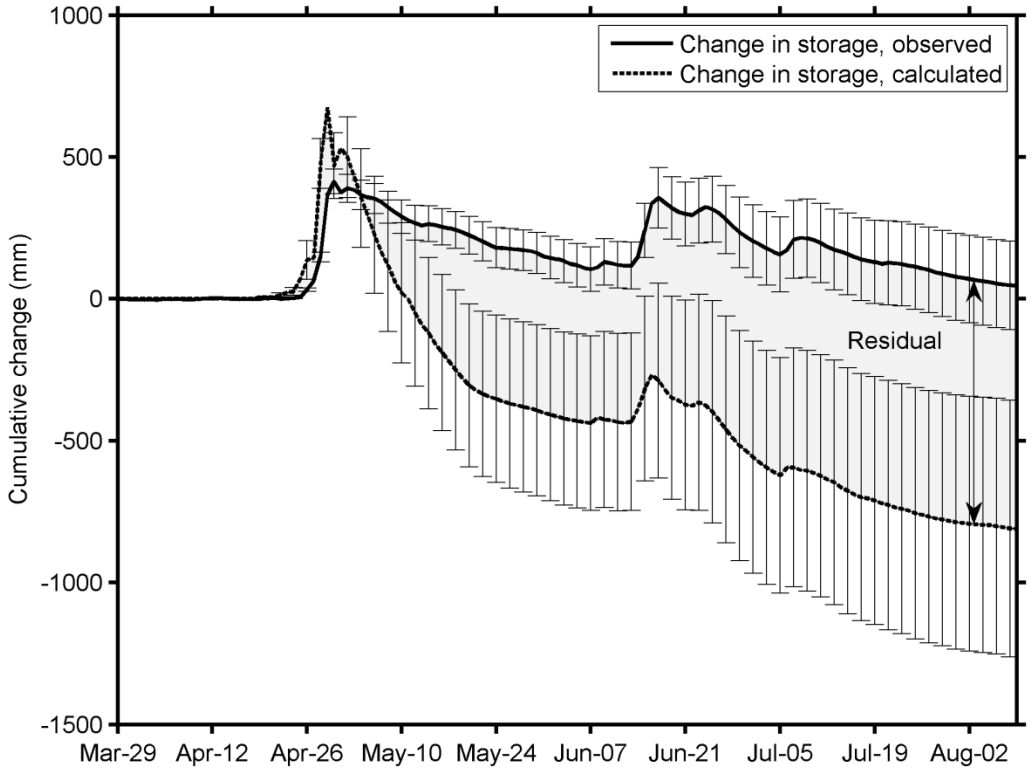

Figure 5.10: Cumulative change in storage in the four reach ponds for spring and summer 2013, both observed and calculated from observations of precipitation, catchment runoff, inflow, evaporation, and discharge. The shaded area indicates the magnitude of the residual between measured and calculated storage change. Error bars indicate the cumulative error estimates based on accuracy of individual water balance terms.

There was a large temporal variation in the residual in response to snowmelt infiltration and rainfall events (Figure 5.11). Local peaks occurred for one to two weeks after peak snowmelt and one to two days after major rainfall events. The recession of the residual flux was similar to the shape of the hydrograph, although it exhibited peaks in the flux as the water table rose and fell. This is consistent with the dynamics of the transmissivity feedback mechanism, where a large increase in lateral flow occurs in transiently saturated, superficial layers (Bishop et al., 2011).

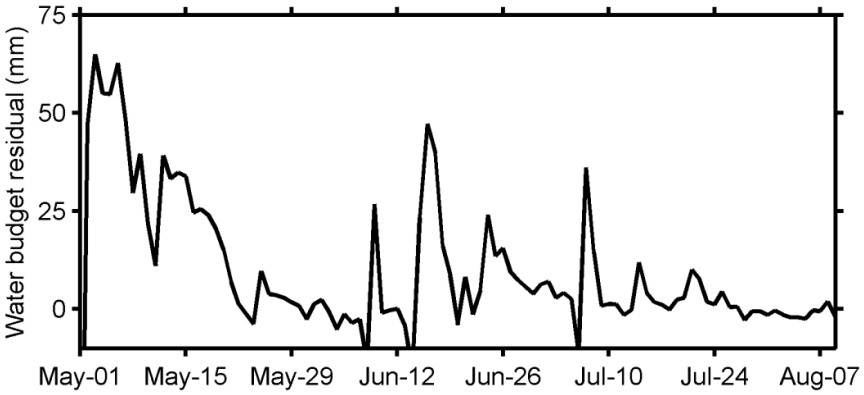

Figure 5.11: Time series of water budget residual for the period 1 May – 9 August 2013.

5.2 Groundwater behaviour

Hydraulic gradients indicate a groundwater flow direction from the hillslopes towards the ponds for the entire study period (Figure 5.12). The water table was closer to the ground surface on the south hillslope adjacent to the pond, due to the presence of a small upslope pond that supplies depression focused recharge, maintaining higher groundwater levels. In the riparian zones and on the south hillslope the water table responded quickly to snowmelt and rainfall, rising to the ground surface leading to fully saturated conditions during and after melt and rainfall events (Figure 5.13). Beneath the north hillslope there was a slower and dampened response, with the water table remaining relatively deep (Figure 5.13). Peak discharge from the basin during spring freshet occurred approximately one week before the piezometers responded on the north hillslope, and two days after piezometers responded on the south hillslope. Peak water table levels on the north hillslope following snowmelt occurred approximately one month after streamflow peaked, and approximately one week after peak streamflow on the south hillslope. During rainfall events, piezometers responded more quickly to inputs, and took approximately one week to reach peak levels on the north hillslope, and peaked the same day or the day before peak streamflow on the south hillslope. Piezometers on the south and north

hillslopes recorded initial water table depths (prior to melt) of roughly 2, 3 and 4 m below ground, and during the study period these water tables rose by roughly 2, 1.5 and 1 m respectively, with lag times increasing with depth, in response to recharge from snowmelt and rainfall (Figure 5.13). This shows the attenuation of the recharge signal by storage in the unsaturated zone.

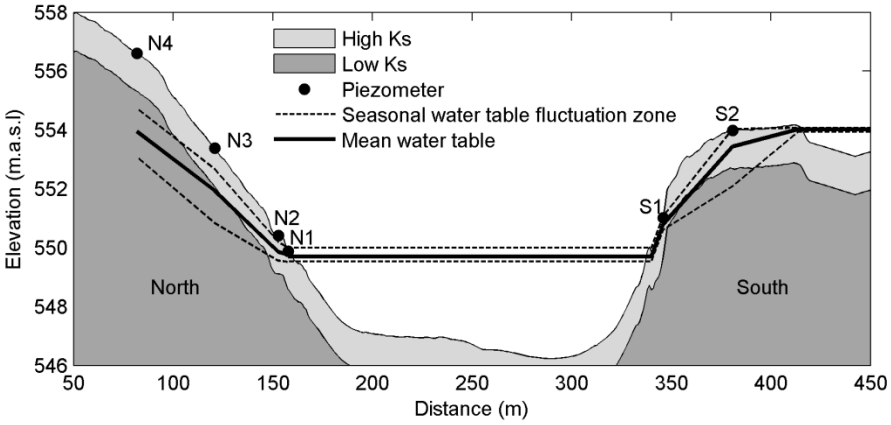

Figure 5.12: Piezometer transect dissecting Pond 125 showing seasonal water table fluctuation and mean water table position for 17 April – 09 August 2013. Pond water levels from Pond 120 are shown in the depression on the far right side of the transect. The lighter gray area is a schematic (not to scale) representation of the fractured and more permeable material near the surface that has greater saturated hydraulic conductivity, K_S.

The water budget residual term was plotted against water table depth measurements from the north and south hillslopes of the piezometer transect (Figure 5.14). Bulk properties (fractures and matrix) of the glacial till measured at SDNWA indicate that the hydraulic conductivity decreases exponentially with depth below ground surface (Figure 3.5) (Hayashi et al., 1997; Bodhinayake and Si, 2004; van der Kamp and Hayashi 2009); therefore, the transmissivity of the till varies with water table depth. For unfrozen conditions, there is an exponential relationship between water table depth on the south hillslope and the water budget residual (Figure 5.14a), suggesting that the residual behaves in a similar manner to what would be expected from a groundwater flux. The exponential relationship between water table depth and residual is not

apparent during frozen conditions or for piezometers on the north hillslope (Figure 5.14b), where the water table is in a deeper position in the till, implying that the north hillslope is decoupled from the reach. The different relationships between the two hillslopes (Figure 5.14) are consistent with the head profiles shown in Figure 5.12. These results imply the water budget residual could represent a net groundwater flux to the ponds, primarily occurring in location such as the south hillslope where the water table was in the shallow effective transmission zone. Water table depths on 9 May, 7 June, and 22 June (Figure 5.15) show that, in general, these locations were those adjacent to upland ponds, the hillslopes between them and the reach ponds, and riparian areas.

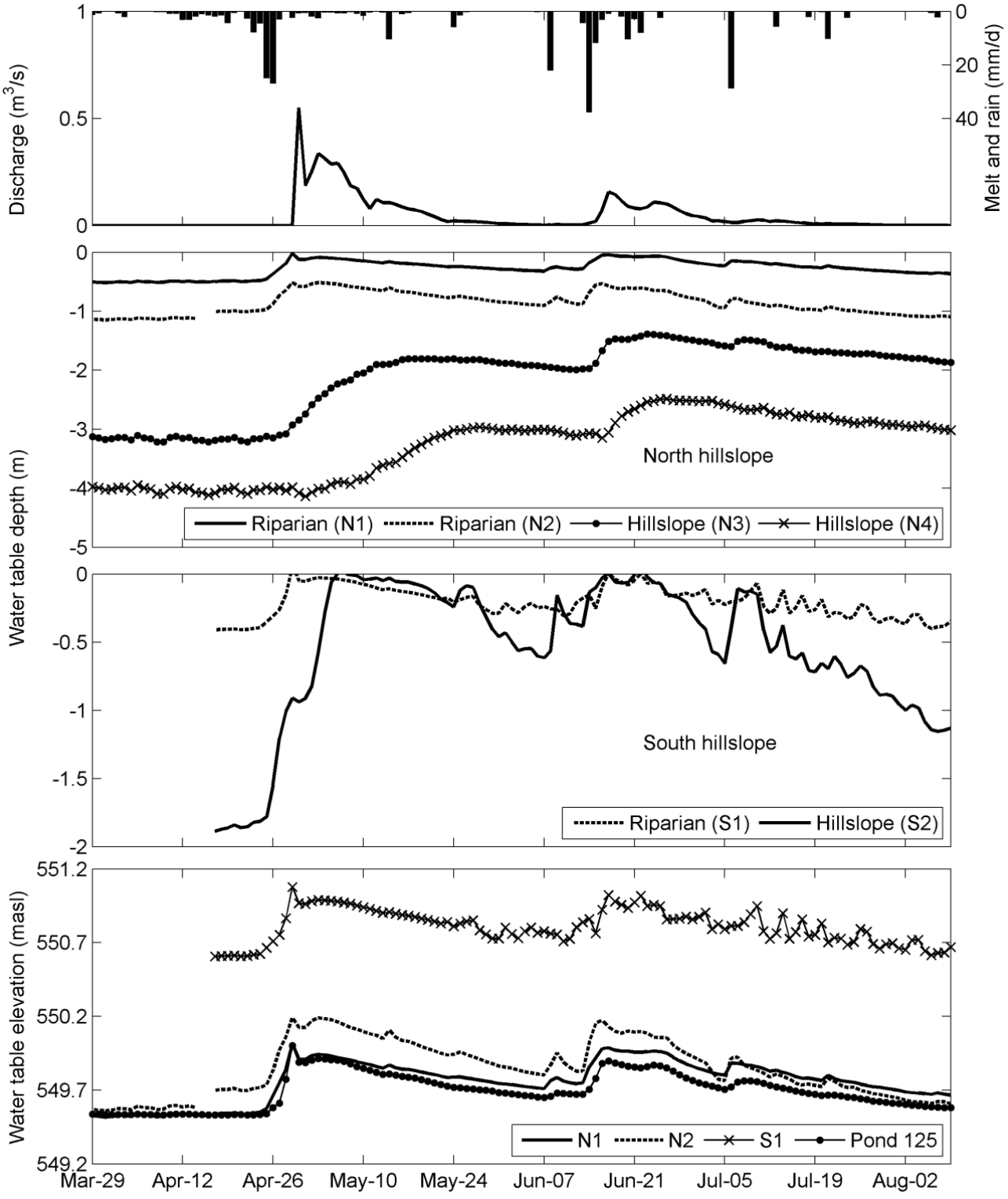

Figure 5.13: Time series of streamflow, precipitation, and water table response on the north and south hillslope of the piezometer transect during spring and summer 2013. Additionally, water table elevation in riparian zones and Pond 125 are included. Piezometer locations are shown in Figure 5.12.

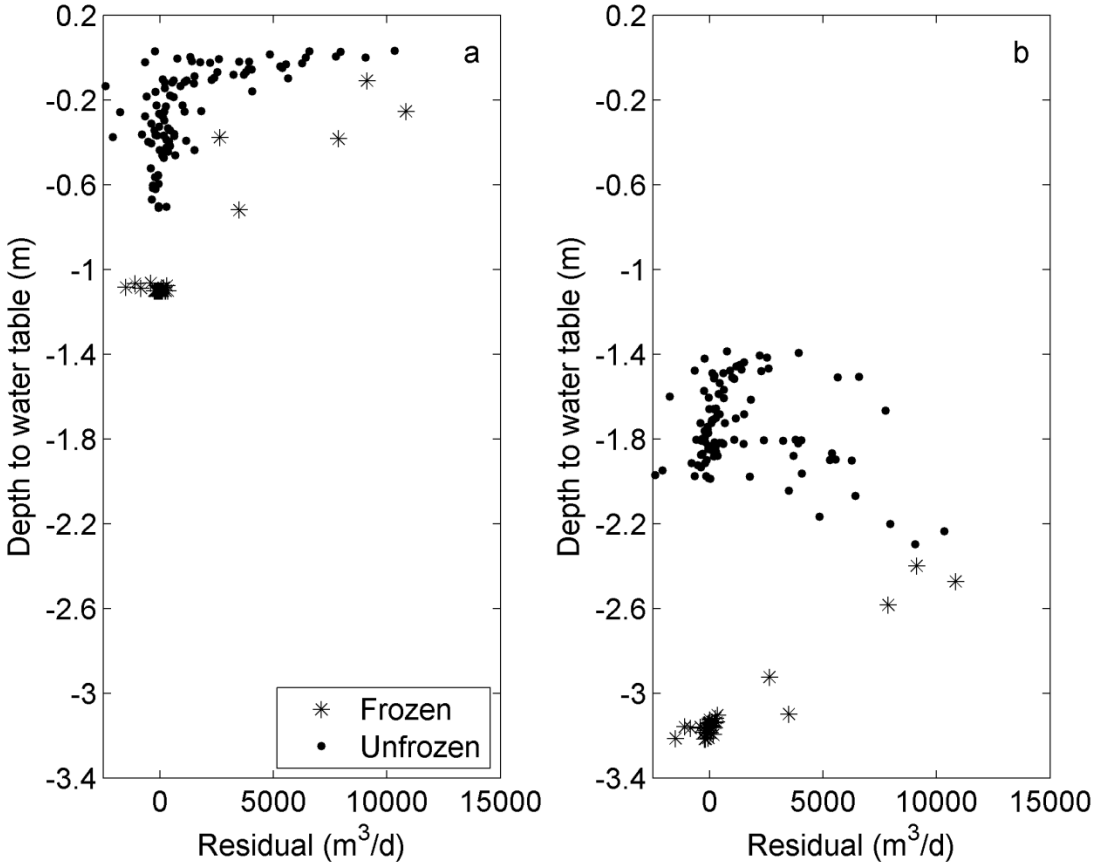

Figure 5.14: Relationship between water budget residual and depth to groundwater for two different locations, a) southern hillslope and b) northern hillslope in 2013. The south hillslope shows an exponential relationship during unfrozen conditions.

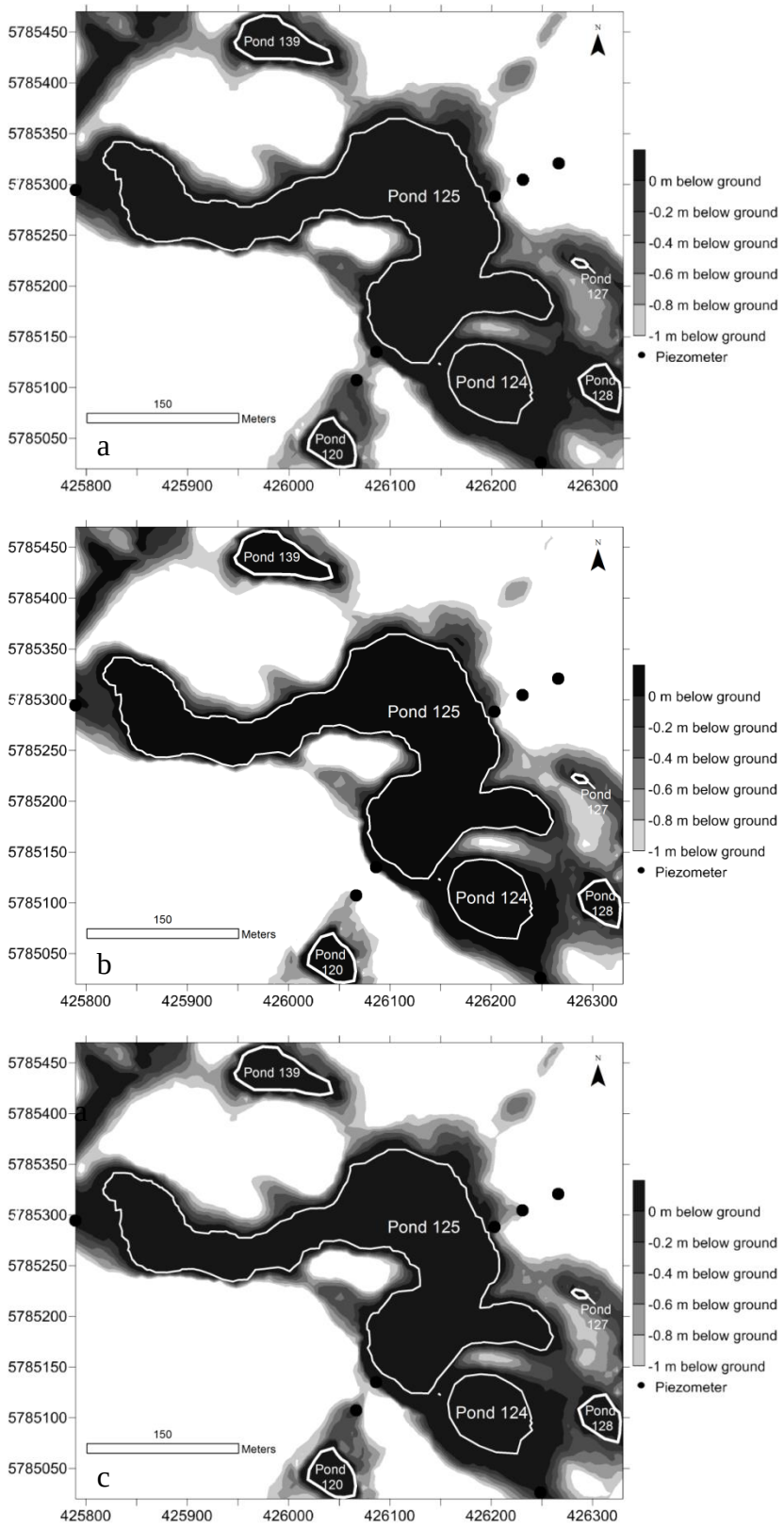

Figure 5.15: Depth to water table (m below surface) on a) 9 May, b) 7 June, and c) 22 June 2013 interpolated from wells and pond levels. The average surface water extent of ponds is outlined.

5.3 Streamflow response

Runoff ratios were highest during the spring freshet and in the latter half of June and much smaller at the end of May, early June, and in July (Table 5.4) as evaporation and discharge losses reduced the storage and degree of connectivity in the reach. The event with the highest runoff ratio of the season, 0.268, was the spring freshet, which was followed by a small event (R/P = 0.068) that was the result of 7.8 mm of rainfall between 24 – 26 May. There was 22 mm of rainfall on 8 June, but this produced very little runoff (R/P = 0.005) and primarily went to refill storage in the catchment. An 83.1 mm pluvial that extended from 13 – 25 June produced a large runoff event mid-summer (R/P = 0.155). This was followed by four events in July where runoff ratios ranged from 0.005 to 0.044.

Field results suggest groundwater was a significant input to reach storage and a notable portion of streamflow response to rainfall inputs. To evaluate the magnitude of the importance of groundwater contribution to streamflow response the runoff ratios for the events described above were calculated using the hydrograph simulated without a groundwater input to reach storage. Simulated runoff ratios without groundwater contributions to pond storage were found to be ~ 65 -75 % of the actual runoff ratios during the two peak events on 30 April and 17 June (Figure 5.16). Overall the variation between hydrographs shows a slight difference in the timing and magnitude of peak streamflow, and a greater discrepancy on the recession limbs. The period between 13 May and 27 May shows the largest difference in streamflow, likely because groundwater maintained surface storage above surface thresholds during this period. The simulated non-groundwater hydrograph in June and July peaked at approximately 0.01 m^3/s less than the observed hydrograph, and recessions were much steeper. The groundwater contribution

served to sustain streamflow into June and July. Without groundwater inputs, streamflow for the season would have ceased 16 days before it was actually observed to stop flowing on 9 August.

Table 5.4: Runoff ratios for five different events during the 2013 study period. P is event rainfall (mm), Qe is event runoff (mm), and Q/P is the runoff ratio.

Event	**P (mm)**	**Qe (mm)**	**Q/P**
Mar 29 - May 23	121.7	32.6	0.268
May 24- May 26	7.8	0.54	0.068
Jun 8	22	0.13	0.005
Jun 13 – Jun 26	83.1	12.95	0.155
July 6	28.8	0.66	0.023
July 13	8.2	0.37	0.044
July 21	10.3	0.07	0.006
July 24	2.4	0.13	0.005

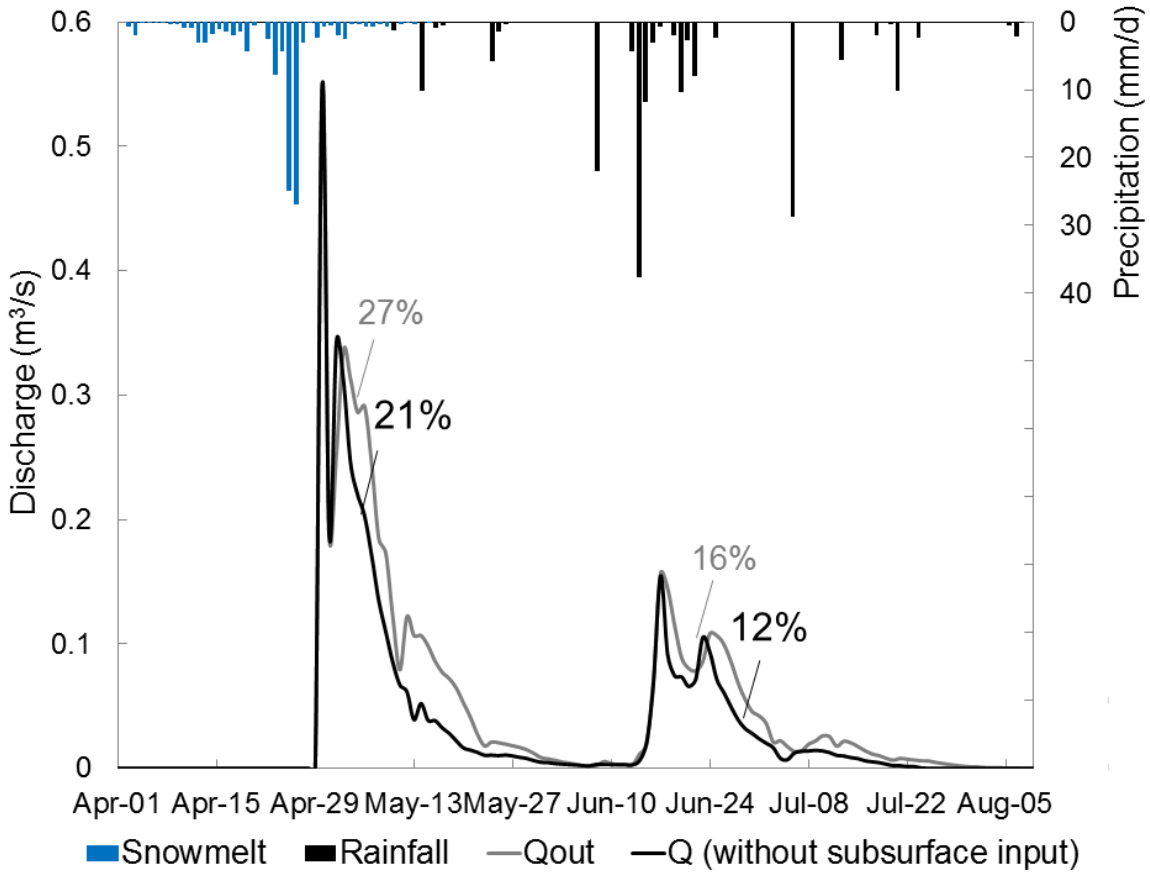

Figure 5.16: Observed (light gray) and modelled (black) discharge, and runoff ratios (Q/P) for snowmelt and rainfall events during 2013.

5.4 Discussion

5.4.1 *Relative importance of subsurface inputs*

The study took place in 2013, which was unusually wet in terms of antecedent pond levels (see Figure 2 in Nachshon et al., 2014), snowpack (the largest in a 24 year record), and June rainfall. However, insights from this period could be important for future conditions, especially since new evidence suggests that precipitation patterns in the Canadian prairies are shifting from primarily convective single-day events to more multi-day rainfall events (Shook and Pomeroy, 2012). Sustained rainfall overwhelms soil storage capacity, leading to groundwater recharge before soil water has opportunity to be consumed by evapotranspiration. This may result in higher water tables and increased rainfall runoff, as was observed during the study period. The low relief and high variability in climatic conditions result in a region that is very responsive to extreme events (Covich et al., 2007; Winter and Rosenberry, 1998).

During periods of high antecedent storage conditions and/or high precipitation inputs, shallow groundwater flow from the hillslopes to the wetlands maintains surface storage, surface connections between ponds, and streamflow. The evidence for this is: *i)* the large groundwater input term from the pond complex water budget; *ii)* the observations of hydraulic gradients towards the ponds coincident with water tables located within the effective transmission zone on the south slope; *iii)* the clear water table responses to recharge following melt and rainfall, followed by water table recessions as the groundwater discharges laterally towards the pond; and *iv)* the strong relationship between the residual water flux (which represents net groundwater exchange) and water table position in hydrologically connected locations. Studies in other catchments underlain with clay rich glacial till have found a similar relationship between subsurface runoff and groundwater storage, where an exponential increase in runoff occurs as

groundwater rises and highly conductive layers are saturated (Rodhe, 1989; Seibert et al., 2003; Detty and McGuire, 2010; Bishop et al., 2011).

These results complement Prairie water budget studies undertaken during drier periods, and indicate a change in predominant hydrological processes during wet conditions. Hayashi et al. (1998) and Woo and Rowsell (1993) both found that snowmelt runoff from uplands and direct precipitation on a closed basin wetland at SDNWA could account for nearly all of wetland inputs. Several studies have found that surface runoff from hillslopes is negligible and that inputs into ponds are only from snowmelt within wetland depressions and riparian vegetation (Pomeroy et al., 2007; Fang et al., 2010). During the study period most of the snowmelt contributing to the ponds originated from grassed hillslopes. Due to higher than average snow accumulation, riparian zones and trees were not the dominant contribution to peak flow as the melt rate was slower than grassed hillslopes and most snow was retained in these covers until after peak flow. These varied results highlight the importance of observations taken across a diversity of climatic conditions when discussing hydrological processes and streamflow regimes.

5.4.2 *Mechanisms of hydrological connectivity*

Hydrological connectivity in this landscape is a transient phenomenon that occurs through both surface and subsurface pathways, particularly in those portions of the landscape downslope from surface storage held in ponds. During the spring freshet when there is sufficient snowmelt, hillslopes become hydrologically connected to the stream/pond network through the process of surface runoff over frozen soils. As soils thaw and infiltrating water is directed to recharging soil moisture deficits the hillslopes cease to contribute surface runoff. Snowmelt runoff often collects in surface depressions, which only permit downslope streamflow once water

levels exceed sill elevations through a process analogous to fill-and-spill (Spence and Woo, 2003) between wetland depressions. After soils thaw, depression focused recharge allows water to seep from the surface storage in ponds to recharge groundwater storage or move to downslope wetlands. This subsurface process is significant to the water budget of downslope wetlands when the water table is within the zone of higher transmissivity.

This sequence of processes implies hydrological connectivity in this landscape is controlled by different factors that influence the timing and magnitude of runoff delivered to the stream. Snowmelt runoff from hillslopes is controlled by the limited infiltration capacity of frozen soils and the timing of delivery of snowmelt (Gray et al., 2001). The process by which surface hydrological connections form among depressions in this landscape is well documented (Winter and Rosenberry, 1998; Leibowitz and Vining, 2003; van der Kamp and Hayashi, 2009; Shaw et al., 2012) and this controls the proportion of the basin that contributes to surface runoff. Subsurface connectivity between hillslopes and wetlands varies with the wetness of the catchment because the direction of groundwater flow is controlled by the water table depth of hillslopes relative to adjacent ponds. Hydraulic gradients directed towards ponds aid in maintaining surface storage, as opposed to drawing on it (e.g. Woo and Rowsell, 1993; Hayashi et al., 1998a). Results here imply there can be a significant contribution of subsurface fluxes to the water budget of a wetland complex under such water table configurations. The concept of an "effective transmission zone", ETZ, which was put forward by van der Kamp and Hayashi (2009), aids in interpreting these observations. The ETZ arises due to the exponential relationship between hydraulic conductivity and depth below ground (Figure 3.5), similar to the transmissivity feedback mechanism (Bishop et al., 2011). When the water table is low, lateral groundwater flow can be considered negligible as the hydraulic conductivity is very small. As

the water table rises, the hydraulic conductivity increases exponentially, such that the same hydraulic gradient can result in large volumes of lateral flow. Above the water table in the unsaturated zone, the hydraulic conductivity is also very low. Thus, the ETZ is a window within the subsurface bounded at the base by the depth of the weathered zone of the till and at the top by the water table. Lateral groundwater flow outside the ETZ (above or below) can be considered negligible.

5.4.3 *Spatio-temporal dynamics of hydrological connectivity between landscape components*

This effective transmission zone is spatially and temporally dynamic, becoming activated when the water table rises, and deactivated when it falls. The groundwater flux into ponds is spatially non-uniform, as demonstrated by contrasting the south and north hillslopes adjacent to Pond 125 (Figure 5.12). Particularly important is the subsurface connection on the south hillslope, where a continuous ETZ between the upslope pond and the lower pond infers a connected subsurface pathway. The map of groundwater depth below ground (Figure 5.15) implies that locations where subsurface connections occur are highly heterogeneous. During the study period, these connections are temporally heterogeneous, yet spatially stable. Temporally, ETZ pathways are expected to develop following snowmelt or rainfall, when there is high antecedent wetness (high water tables and pond levels). Spatially, ETZ pathways are expected to develop between adjacent wetlands, and the closer the wetlands are together, the more significant the pathway.

The results of this analysis are limited to a 1 km^2 catchment within a hummocky area of the Prairie Pothole Region. The deposition of glacial till was unevenly distributed throughout the PPR, which consists of different morphologies of glacial drift, including end moraines, ground

moraines, outwash plains, and lake plains. Therefore, there are varying degrees of topographic relief in the region (Winter, 1989). Relief generally decreases from west to east in the PPR. The west of the region (Missouri Coteau) contains large end moraines where local relief can be anywhere between 15-45 m from hilltop to depression. These areas generally have deep wetlands, with little integrated drainage (Leibowitz and Vining, 2003; Winter, 1989). The easternmost portion of the PPR is relatively flat glacial lake bed (Lake Agassiz). Water ponds easily on the silty clay deposits and drainage networks are generally more integrated over larger areas. Between the two extremes is an intermediate level of drainage where the local relief from hilltop to depression may be only a few meters.

Darcy's Law indicates that for head gradients twice as large we should expect groundwater fluxes of twice the volume, and vice versa for smaller gradients. The importance of groundwater flux to the surface water budget of wetland complexes outside of the intermediate region of the PPR may therefore be lesser or greater than the results of this study indicate. While there is more potential for water to travel downslope in the west of the PPR, wetlands are more separated due to larger moraines that could limit the extent of the ETZ. Conversely, in eastern parts of the PPR there is less potential energy for transporting water downslope because the topography is much less steep, which may also limit the magnitude and importance of a groundwater flux.

Land-use may also be an important consideration when transferring the results of this study to other regions in the PPR. For instance, van der Kamp et al. (2003) found that infiltration is much greater in uncultivated soils under both frozen and unfrozen conditions. This can limit the amount of surface runoff produced in grassed areas and may increase the importance of subsurface transfer of water because increased infiltration may result in higher groundwater

tables. Furthermore, hydraulic conductivity is expected to be much higher near the surface in undisturbed soils, as the process of tilling breaks up macropores and condenses weathered soil. Since European settlement the PPR has been experiencing drainage to the extent that 50-75% of wetlands in some areas have been drained (Gleason and Euliss, 1998). The storage of water in wetlands is essential to the spatial extent of the ETZ because water retained in ponds increases groundwater infiltration and maintains high water tables needed to transmit water efficiently in the subsurface. Drainage may lessen the groundwater flux necessary for maintaining surface storage that is important for streamflow generation in Prairie basins.

There are many characteristics of a catchment that can affect how water is redistributed across space and time. Differing runoff regimes are driven by the heterogeneous behaviour of the landscape in space and time. The different piezometer responses across this catchment indicate that different areas in the catchment contribute disproportionately to runoff under certain conditions. This suggests that source areas can be predicted in part based on landscape structure in prairie pothole catchments. Many studies have investigated the relationships between landscape topography, spatial sources of runoff, and runoff generation, and have observed that the factors governing runoff response change in time according to catchment wetness state (Dunne and Black, 1970; Sidle et al., 2000; McGlynn and McDonnell, 2003; Jencso et al., 2009; Jencso et al., 2011). Catchments can exhibit non-linear or threshold behaviour in discharge when runoff producing mechanisms or source areas are activated under wet conditions (Detty and McGuire, 2010). This is attributed to the expansion of contributing area that occurs when there is increased connectivity between saturated surface or subsurface areas (Sidle et al., 2001; Detty and McGuire, 2010). During the study period, the connected areas did not vary much throughout the summer period (Figure 5.15). Above average snowfall and June rainfall suggest that the

observed period of connectivity between wetlands was more prolonged than during a “normal” precipitation year. Rarely on record have conditions been wet enough over a sustained period to generate flow of such long duration as observed in 2013; therefore, the hydrologic processes currently being measured here are representative of the functioning of certain prairie wetland catchments under very wet conditions.

CHAPTER 6 : SIMULATING THE WATER BUDGET OF A WETLAND COMPLEX

This chapter describes the results of the modelling experiment that was introduced in Chapter 4. The identifiability of model parameters, the model performance relative to observed discharge and pond levels, and insights from the experiment are discussed.

6.1 Model calibration

The model calibration considered the performance of the model with respect to daily discharge data. Independent simulations of discharge showed a wide range of responses. An RMSE threshold of 2000 m^3 was chosen based on visual assessment of the discharge curves; simulations with RMSE values below this threshold were considered behavioural. The spread of cumulative and daily discharge curves was large, even within the bounds of behavioural realizations (Figure 6.1). Cumulative discharges in these realizations ranged from 84% to 105% of the observed cumulative discharge. The model generally reproduced the shape of the hydrograph, although the rainfall runoff responses were too flashy, especially after day 100. The initial streamflow peak following snowmelt was simulated well; the behavioural simulations showed good timing for estimating the peak daily discharge. Simulated peak daily discharge ranged from 0.477 m^3/s to 0.611 m^3/s, or 87% and 111% of the observed value (0.550 m^3/s), respectively. Many realizations in Figure 6.1 underestimated spring discharge, but overestimated summer discharge, and thus the cumulative discharge for the study period was similar to observed. The discrepancies between observed and simulated rainfall runoff responses suggest that the model allowed too much surface runoff to occur during these periods, likely because alpha was fixed for different events.

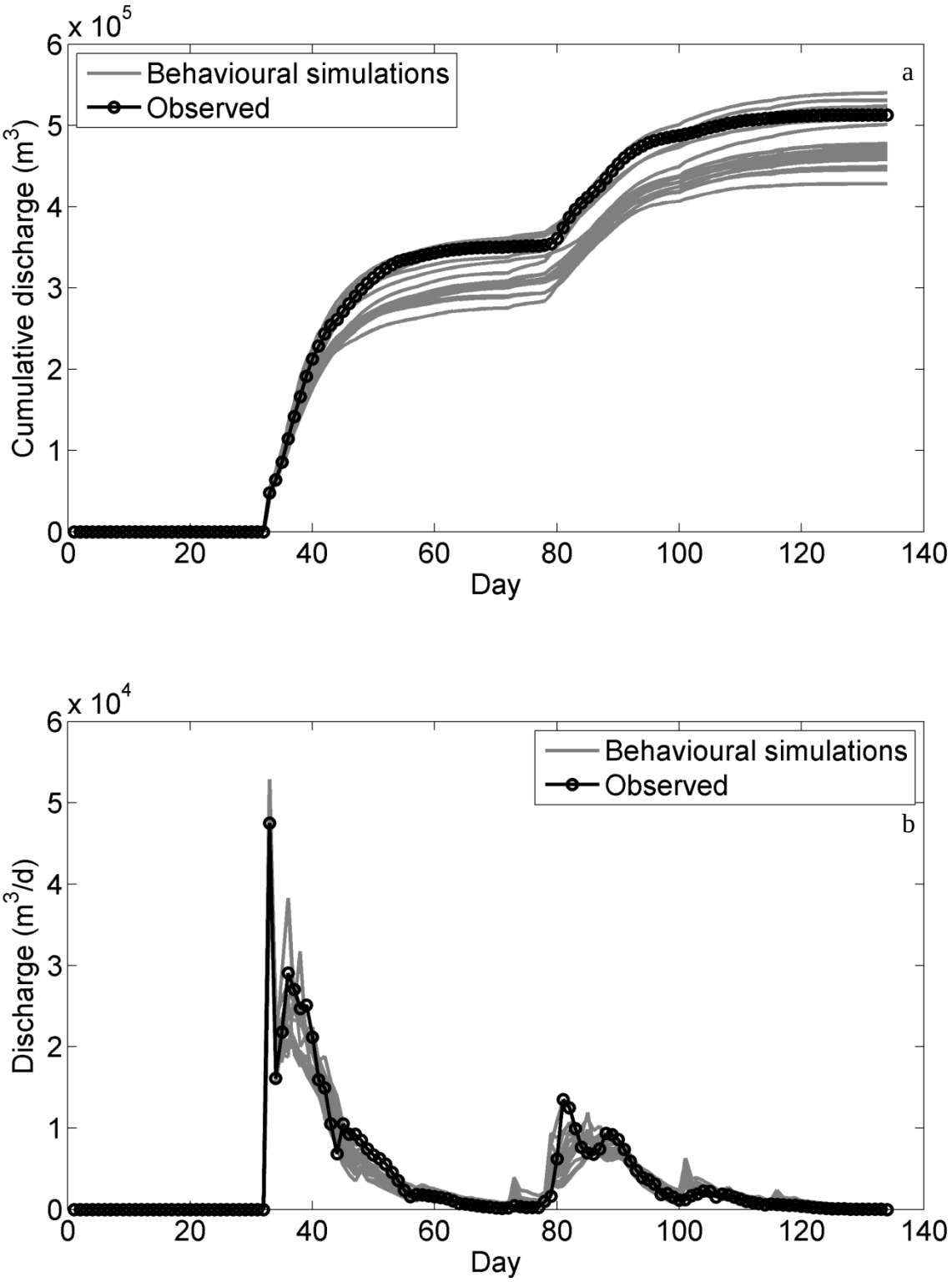

Figure 6.1: Model outputs of discharge for behavioural realizations in gray, and observed a) cumulative and b) daily discharge in black.

The model comprises fourteen parameters whose values are unknown. To explore whether the model is a plausible representation of the system and the implications of uncertainties in model parameters a Monte Carlo analysis was performed using 100,000 simulations. All parameters were varied simultaneously in each of the realizations and results are shown as dotty plots in Figure 6.2, Figure 6.3, Figure 6.4. Dotty plots are used to visualize how the performance of the model depends on different combinations of parameters. The model performance can be described as an n-dimensional objective function surface, where n is the number of free parameters. The dotty plots are a projection of the n-dimensional surface into one parameter dimension. The y-axis for all subplots is the RMSE value (to be minimized) and the x-axis corresponds to values of randomly sampled parameters. If the surface of the dotty plot has a well-defined minimum RMSE value, then the parameter is considered to be well identified (Beven, 2012).

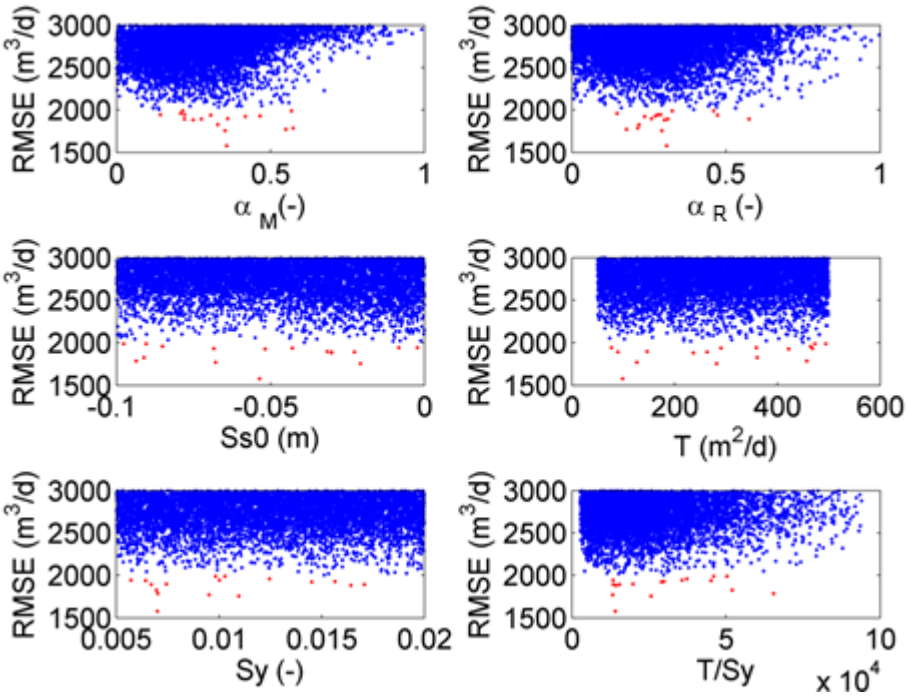

Figure 6.2: Dotty plots of model performance (RMSE to be minimized) against parameter values for 100,000 model realizations in blue, and behavioural realizations (RMSE < 2000) in red.

The runoff partitioning parameters, α_M and α_R, are more strongly identifiable than the initial soil moisture content, S_{s0}, or the aquifer properties, T and S_y (Figure 6.2). Transmissivity and specific yield in part determine the groundwater flux, and the ratio of the two (the hydraulic diffusivity) is somewhat more identifiable than each parameter considered separately because combinations of a relatively large specific yield and small transmissivity produce the same groundwater flux as small specific yield and large transmissivity.

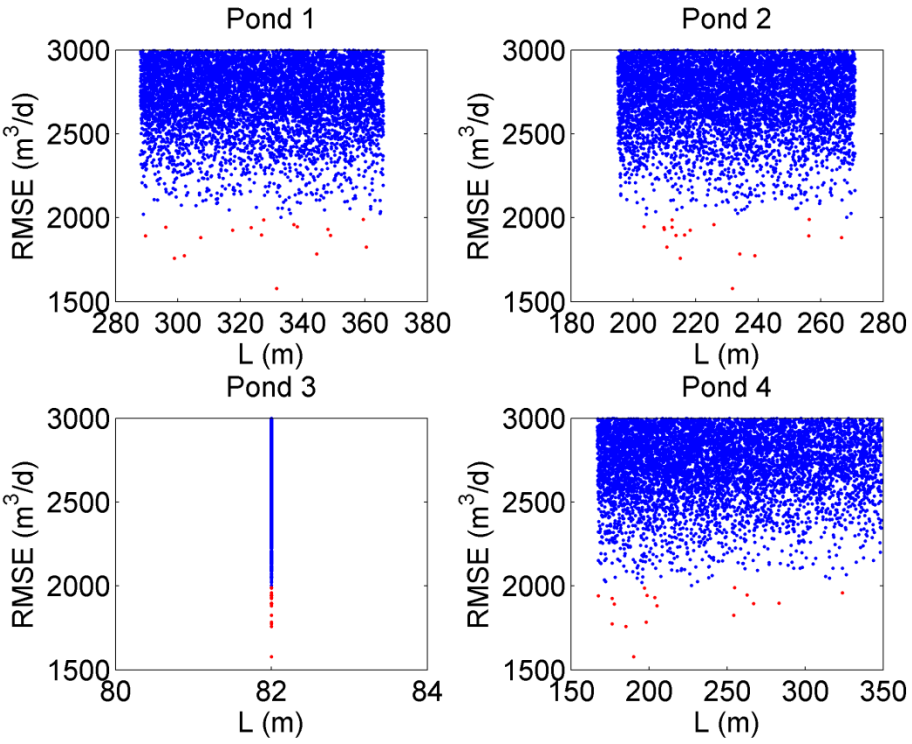

Figure 6.3: Dotty plots of model performance (RMSE to be minimized) against hillslope length, L, values for 100,000 model realizations in blue, and behavioural realizations (RMSE < 2000) in red.

The hillslope length parameter represents the contributing area of each pond. The optimum hillslope length parameter set is somewhat isolated, suggesting that a larger number of realizations could be potentially beneficial (Figure 6.3). However, for Ponds 2 and 4 there is some shape in the dotty plots. The parameters in the middle of the range of hillslope lengths for

Pond 2, and the smaller end of the range for Pond 4 produce a slightly better fit to observed discharge. The storage-discharge coefficients, a and b, determine the rate of water discharged from each pond and are quite identifiable (Figure 6.4). This relationship was fixed for Pond 4 as observations of pond storage and discharge were available to determine the power law relationship for Pond 4.

Overall the dotty plots demonstrate that the model cannot be well identified by this analysis. With the exception of the runoff partitioning parameters, the range of behavioural simulations cover the whole range of parameters sampled. There were too many parameters and too few realizations to adequately determine the parameter surface, and the Monte Carlo simulation was too computationally expensive to feasibly include more runs in this study.

6.2 Model performance

The performance of the model in accurately simulating state variables of the three stores (pond, groundwater, and soil) was also assessed. The pond levels for those discharges in Figure 6.1 have a wide range (Figure 6.5). The same outflow can be produced for many different pond levels by varying the storage-discharge parameters, so the level is only constrained by the discharge for Pond 4 where the relationship between storage and discharge is fixed. Because an overly large inflow can be compensated by an overly large outflow without changing pond level, the pond levels were not a sufficient measure by which to calibrate the model. To correctly simulate the initial rise in pond level during the snowmelt period and the timing of the onset of discharge, a "snow-dam" threshold had to be included as a fixed parameter in the model. This threshold is greater than the topographically defined spill threshold and was observed in the field to exert an important control on the dynamics of pond and streamflow hydrographs.

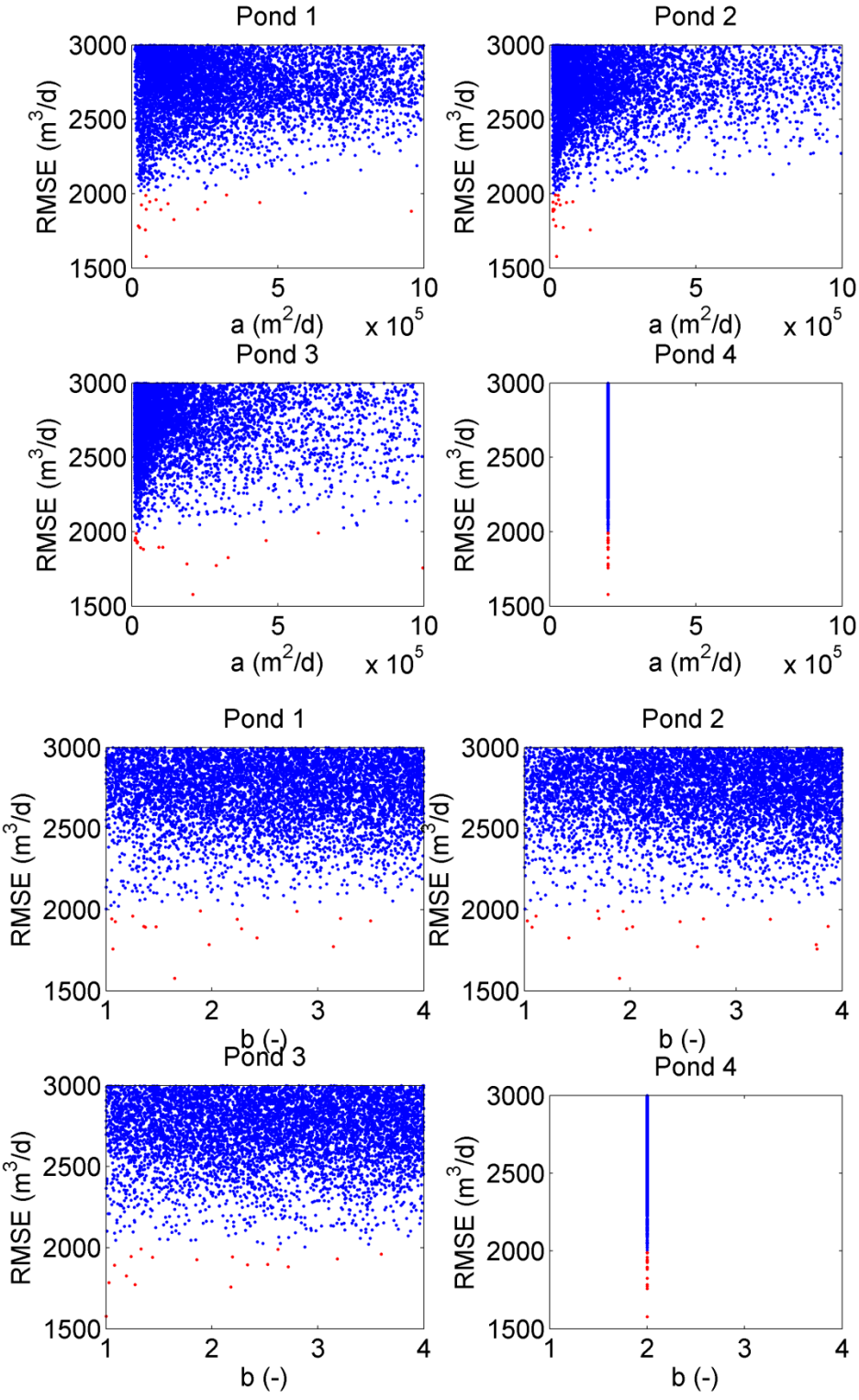

Figure 6.4: Dotty plots of model performance (RMSE to be minimized) against storage-discharge relationship coefficients, a and b, for 100,000 model realizations in blue, and behavioural realizations (RMSE < 2000) in red.

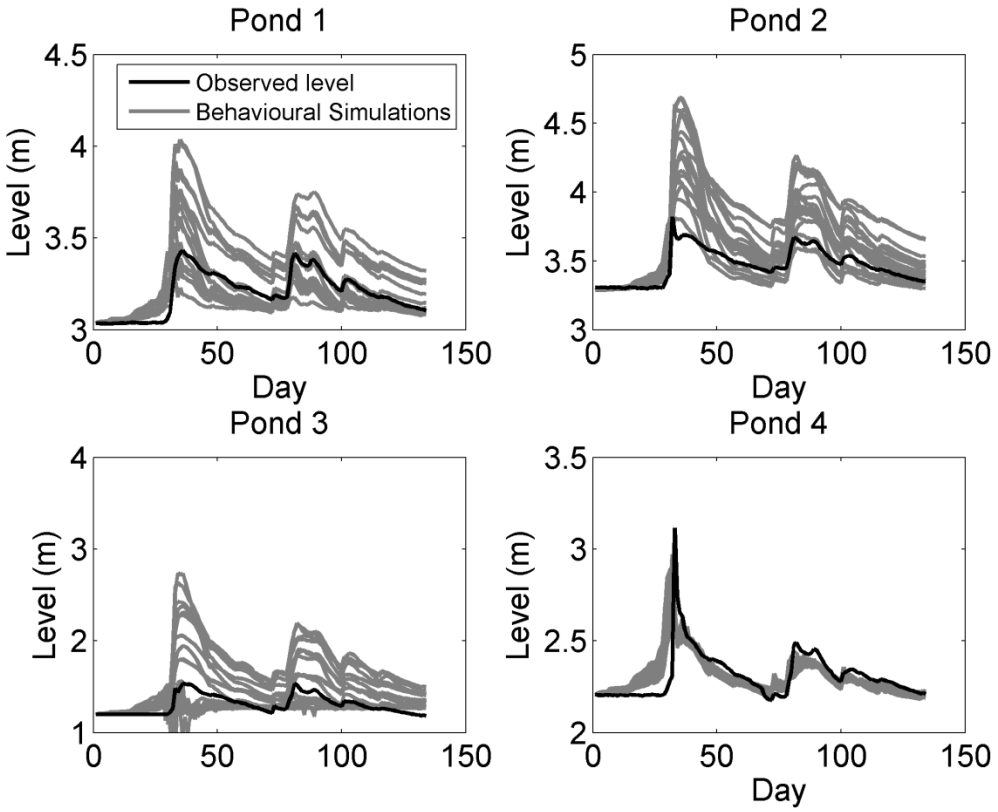

Figure 6.5: Modelled pond levels of behavioural realizations in gray, and observed pond levels in black.

The simulated groundwater responses were quite varied, where different realizations had opposite groundwater behaviour for similar cumulative flows (Figure 6.6). Generally, field observations indicate an increase in groundwater levels following snowmelt and rainfall events (Figure 5.13). However, in some simulations the difference between groundwater level, h_g, and pond level, h_p, was negative, indicating that the model fit the observed discharge better when the ponds were able to lose water to the groundwater store. These simulations are not broadly consistent with observations. Therefore, simulations where the cumulative groundwater flux was less than zero were rejected. The difference in distributions of α_M between behavioural and rejected simulations illustrates that when the volume of surface snowmelt runoff was large, the ponds filled to a level higher than the groundwater store, which backfilled the groundwater store

(Figure 6.7). There is a lot of spread in the α_M values because many parameters influence the magnitude of the groundwater flux.

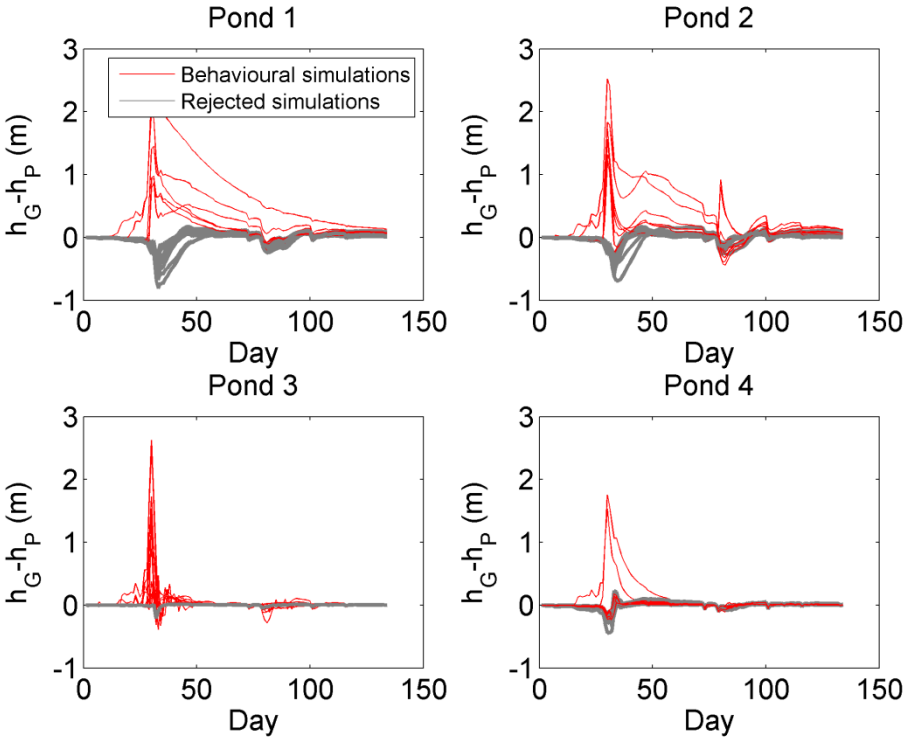

Figure 6.6: Modelled groundwater levels of behavioural realizations relative to pond levels. Positive cumulative groundwater fluxes are shown in red, and negative cumulative groundwater fluxes in gray.

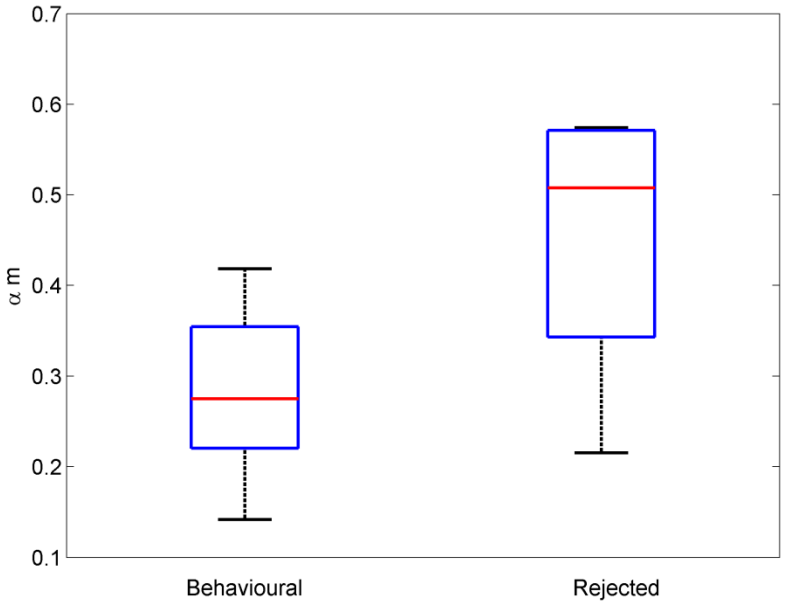

Figure 6.7: Distribution of snowmelt runoff partitioning parameter, α_M, for behavioural and rejected simulations.

The Pond 2 saturated zone store was the only one that showed significant recharge from rainfall events beginning on approximately day 75. This occurred in simulations when the area of the upland stores was relatively large compared to the area of Pond 2 (Figure 6.6). Although all hillslope units have identical transmission parameters (i.e. Sy, T, and FC), the saturated zone response varied for different ponds because hillslope length and pond circumference were based on individual hillslope-pond unit areas. As defined in the model structure, recharge to the groundwater store from the unsaturated zone only occurs when field capacity in the soil moisture store is exceeded. Precipitation entering the soil moisture bucket that exceeds field capacity goes directly into groundwater storage. The unsaturated zone storage (Figure 6.8) shows that soil moisture only exceeded field capacity during the rainfall events (~ day 75-100) in the Pond 2 hillslope. Thus, for the most part there was very little recharge to the saturated store because

there was no way to increase the groundwater levels without inputs of snowmelt or rainfall except when the hydraulic gradient reversed.

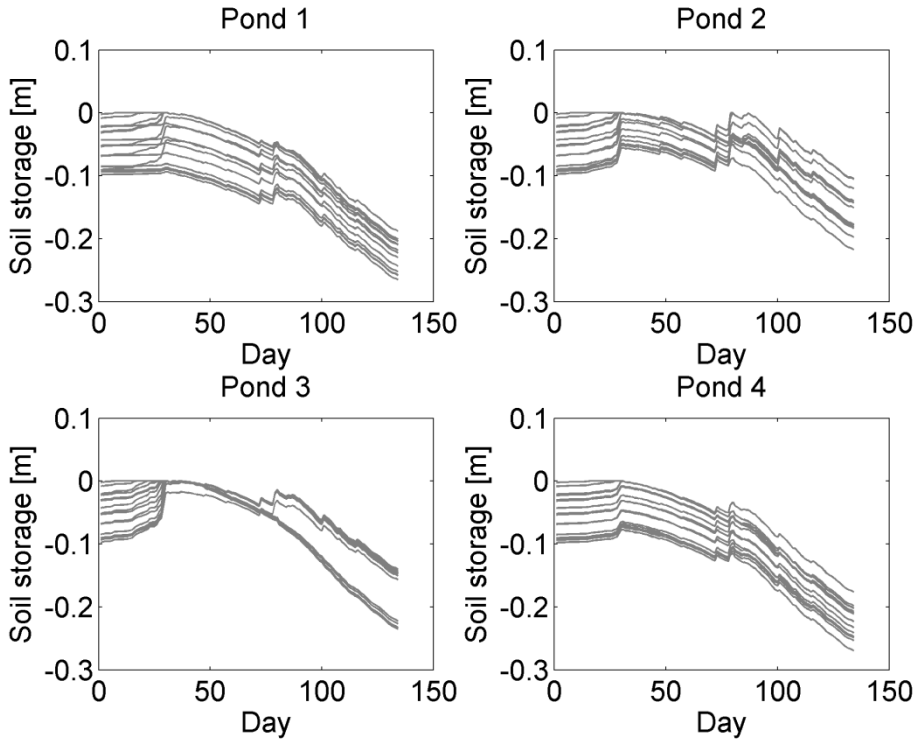

Figure 6.8: Top 0.1% of modelled soil moisture storage based on RMSE.

6.3 Discussion

6.3.1 *Strengths and limitations of modelling approach*

Although the model was able to simulate observed streamflow, there are several significant limitations in the model structure that prevent its use in determining dominant hydrological processes in the catchment. The modelling experiment indicates there are failings with respect to underlying assumptions of the system in the model structure. However, this exercise has provided a number of insights into the challenges associated with modelling a prairie wetland complex. In general, the dynamics of rainfall runoff events are not well captured

by the model. The model allowed too much surface runoff to occur during rainfall, as indicated by the peaks in streamflow during rainfall events that did not occur in the observed flow. The range of groundwater and surface runoff fluxes suggests that when the volume of surface runoff was large, it was compensated for by losing water from the ponds to groundwater to match observed streamflow. The reversal of hydraulic gradients has been observed in many closed basin wetland field studies in this region (Winter and Rosenberry, 1995; Hayashi et al., 1998a), although observations indicate that this phenomenon did not occur during the study period. The peaks in streamflow from rainfall runoff also suggest that the rainfall signal must be lagged longer to accurately simulate the observed hydrograph. Several studies have described the importance of upland ponds in storing water in this landscape, which is then released over a period of several days to weeks over the surface (Shaw et al., 2012) and through the subsurface (Chapter 5; van der Kamp and Hayashi, 2009). The data requirements of the model are too extensive to practically include discrete units for all the ponds in the watershed; thus, all upland ponds were lumped into a single hillslope unit for each of the major ponds. In reality, the contributing area varies both between and during runoff events and is controlled by the storage capacities of individual ponds in the catchment (Shaw et al., 2012). However, this behaviour is difficult to simulate given the large data requirements for solving such a highly distributed problem where each pond's storage is a separate state variable (Shook and Pomeroy, 2011; Huang et al., 2013; Shaw et al., 2011).

A consequence of this problem is that the model does not account for surface runoff from upland ponds that occurs on days when there is no precipitation or melt input. The groundwater store is the only way that the hillslope unit can store water and release it to the reach ponds gradually. However, due to using a fixed transmissivity value for the whole landscape, the

groundwater store cannot transmit water quickly enough to account for rapid surface and subsurface runoff and also maintain high enough levels to sustain flow into the recession periods. The exclusion of an upland store that sustains groundwater levels seems to be a significant problem in modelling the groundwater levels and surface runoff in the catchment. A more complex structure may be required to encompass sub-grid processes. Some prairie modelling efforts have had success using semi-distributed Hydrological Response Units (HRUs) (e.g. Fang et al., 2010). However, these models are potentially difficult and time consuming to parameterize and may currently be better suited to operational applications as opposed to the type of thought experiment that was the aim of this study.

There are also several limitations to the parameterization of the model. As described above, the runoff-partitioning parameters do not have sufficient flexibility to adequately simulate different rainfall runoff events if the contributing area remains fixed. Furthermore to reduce complexity in the model and the number of parameters to be calibrated, a single value of transmissivity was used for calculating the groundwater flux. Although the soil moisture store does exert a threshold control on groundwater response, as it is only when the soil is at field capacity that the groundwater store is recharged, this may not be adequate to simulate the non-linear runoff response in groundwater flow as was observed in Chapter 5. It is not clear whether including a varying transmissivity with water table height, as was observed in the field would aid in simulating the dynamics of groundwater flow, and this remains to be explored in further work.

Another issue with the model parameterization is the sensitivity of the storage-discharge relationships in controlling streamflow. To calibrate the model using pond level, the storage-discharge relationship parameters must be known if the size of the catchment varies between realizations, or else the model will produce too wide a range of discharges that may still be

classified as “behavioural”. Furthermore, if the relationship is not defined, the hillslope length parameter cannot be identified from the flow measurements (Figure 6.3).

Lastly, the number of free parameters (n=14) is too high to sample the parameter space efficiently and effectively. The Monte Carlo method is most effective when 10^n model realizations are run, where n is the number of parameters to be calibrated (Beven, 2012). Performing this many runs is too computationally expensive to complete within a realistic timeframe. However, the model is a useful conservative mass balance model that can simulate both surface and subsurface processes. Thus, by altering parameters it is possible to discern the effect different values have, not only on the water budget of an individual pond, but on integrated catchment discharge. A more complicated, physically-based modelling structure including more upland landscape units may be able to represent the hydrology of the catchment better. Fang et al. (2010) were able to simulate snow dynamics and streamflow in a prairie pothole watershed using the Cold Regions Hydrological Model, although it is unclear if this would result in more accurate streamflow simulation in the study catchment.

6.3.2 *Modelling experiment*

The limitations of the modelling structure inhibit explicitly testing the hypothesis that groundwater flux sustains pond levels and, in turn, streamflow. However, this preliminary modelling effort does provide some further justification for several conclusions from the field study described in Chapter 5. The model can evaluate the different ranges of possibilities in the water budget under different melt partitioning (melt vs. runoff) scenarios. Although the range of model outputs does not definitively determine the proportion of snowmelt that infiltrated into the soil, the behavioural realizations describe behaviour that is consistent with significant infiltration

into frozen soils. In Chapter 5 this was assumed based on the application of the Gray model; however, here we have shown that low infiltration rates (i.e. less than ~ 50%, Figure 6.2) result in large volumes of rapid surface runoff to the ponds, which reverses the hydraulic gradients between ponds and uplands, so that the ponds recharge the groundwater laterally. This behaviour is inconsistent with field observations.

Other insights are the importance of including a pond spill threshold and a snow dam threshold, and a unique storage discharge relationships for determining accurate outflow from individual wetlands. Snow damming at the pond outlet, which retains water in wetland depressions above the level of the topographically defined spill threshold, was shown to be important to both the timing and magnitude of peak discharge both in the model and field study. Snow dams are a common feature in channels in the high arctic and have a significant impact on fluvial processes in those regions (Woo and Sauriol, 1981). However, these effects are not commonly discussed in studies of prairie pothole catchments.

An additional insight from this exercise was that pond level was an ineffectual observation for constraining the volume of streamflow in the model. Though many studies have used this as a measure by which to gauge the performance of a model in generating runoff (e.g., Su et al., 2000; Krasnostein and Oldham, 2004), these were studies of individual wetlands. Unless either the storage-discharge parameters or all other fluxes to and from the pond are known, the pond level cannot be used to calibrate the model because there will be a large variation in possible discharges. This suggests that for models based at the sub-basin scale storage-discharge parameters are essential observations for properly determining the water budget when the contributing area is unknown. Frequently, however, we lack knowledge of these relationships. Establishing stage-discharge relationships for individual wetlands will provide

similar advantages to using V-A-h relationships (van der Kamp and Hayashi, 2000) in modelling prairie wetlands.

CHAPTER 7 : CONCLUSIONS

In this thesis observations from wetlands and groundwater in the Canadian Prairie Pothole Region were interpreted to provide insights into the hydrological processes under unusually wet conditions. Previous studies in this and other Prairie Pothole catchments have not documented subsurface fluxes as a factor in maintaining surface storage and surface connections. Results presented here show that during wet conditions, shallow groundwater flow to a wetland complex can maintain surface storage, surface connections, and streamflow. Subsurface connectivity was via flow pathways through the effective transmission zone, which is spatially and temporally dynamic. Areas where the effective transmission zone was activated were found to be highly heterogeneous, but were focused around the riparian zone of the ponds and downslope from ponds. Where two ponds are adjacent to one another, the effective transmission zone may potentially form a continuous subsurface connection between the ponds. The activation of the effective transmission zone depends critically on the antecedent water table depth. As such this mechanism is less likely to be significant under drier conditions, and in locations away from surface storage. Thus, both the topology of landscape elements and antecedent storage conditions are a primary control on the transfer of water to the basin outlet. This mechanism has been described previously (van der Kamp and Hayashi, 2009), but this is the first time that it has been shown to be important for sustaining streamflow.

A modelling experiment was developed to evaluate the hydrological behaviour in a hillslope-pond complex. Results show that the model was capable of simulating basin streamflow, and pond-groundwater interactions that included reversals in hydraulic gradient, but that a simple structure of coupled hillslope-pond units was not adequate for simulating the variety of hydrological processes observed in the catchment. The model experiment did not

explicitly take into account upland pond storage, but field results suggest that including more landscape units may aid in simulating rainfall runoff processes. The modelling experiment provided several other insights that will aid in future modelling work in this region. To use pond level observations to constrain the volume of surface and subsurface runoff from uplands to surface storage in ponds, storage-discharge relationships are required for individual ponds

These findings have important implications for understanding flood risk in the prairies because under wetter conditions an additional streamflow generation mechanism can be become activated that is often considered to be insignificant even under such conditions. This may not have a large impact on peak flows in headwater catchments, but is likely to lead to sustained flow from the ephemeral streams into the larger drainage networks. There is a need to continue developing modelling tools to handle these processes in flood risk and water resources models.

REFERENCES

Armstrong R, Pomeroy JW, Martz LW. 2008. Evaluation of three evaporation estimation methods in a Canadian prairie landscape. *Hydrological Processes* **22:** 2801–2815.

Baldocchi DD, Hicks BB, Meyers TP. 1988. Measuring biosphere–atmosphere exchanges of biologically related gases with micrometeorological methods. *Ecology* **69**: 1331–1340.

Beven K. 2012. Parameter Estimation and Predictive Uncertainty. In *Rainfall-runoff modelling: the primer*. Second Edition. John Wiley & Sons, Ltd.: Chichester, UK.

Bishop K, Seibert J, Nyberg L, Rodhe A. 2011. Water storage in a till catchment. II: Implications of transmissivity feedback for flow paths and turnover times. *Hydrological Processes* **25**: 3950–3959. DOI: 10.1002/hyp.8355.

Blanken PD, Rouse WR, Culf AD, Spence C, Boudreau LD, Jasper JN, Kochtubajda B, Schertzer WM, Marsh P, Verseghy D. 2000. Eddy covariance measurements of evaporation from Great Slave, Northwest Territories, Canada. *Water Resources Research* **36**(4): 1069

Buttle J, Dillon P, Eerkes G. 2004. Hydrologic coupling of slopes, riparian zones and streams: an example from the Canadian Shield. Journal of Hydrology **287**: 161–177. DOI: 10.1016/j.jhydrol.2003.09.0221077.

Bodhinayake W, Si BC. 2004. Near-saturated surface soil hydraulic properties under different land uses in the St Denis National Wildlife Area, Saskatchewan, Canada. *Hydrological Processes* **18**: 2835–2850. DOI: 10.1002/hyp.1497.

Bracken L, Croke J. 2007. The concept of hydrological connectivity and its contribution to understanding runoff-dominated geomorphic systems. *Hydrological Processes* **21**: 1749–1763. DOI: 10.1002/hyp.

Bracken LJ, Wainwright J, Ali G, Tetzlaff D, Smith MW, Reaney SM, Roy AG. 2013. Concepts of hydrological connectivity: Research approaches, pathways and future agendas. *Earth-Science Reviews* **119**: 17–34. DOI: 10.1016/j.earscirev.2013.02.001.

Cook B, Hauer F. 2007. Effects of hydrologic connectivity on water chemistry, soils, and vegetation structure and function in an intermontane depressional wetland landscape. *Wetlands* **27**(3): 719–738.

Covich AP, Fritz SC, Lamb PJ, Marzolf RD, Matthews WJ, Poiani KA, Prepas EE, Richman MB, Winter TC. 1997. Potential effects of climate change on aquatic ecosystems of the Great Plains of North America. *Hydrological Processes* **11**: 993–1021.

Dunne T, Black, RD. 1970. Partial area contributions to storm runoff in a small New England watershed. *Water Resources Research* **6**(5): 1296–1311. DOI: 10.1029/WR006i005p01296.

Detty JM, McGuire KJ. 2010. Threshold changes in storm runoff generation at a till-mantled headwater catchment. *Water Resources Research* **46**: W07525. DOI: 10.1029/2009WR008102.

Devito KJ, Hill AR, Roulet N. 1996. Groundwater-surface water interactions in headwater forested wetlands of the Canadian Shield. *Journal of Hydrology* **181**: 127–147.

Dingman SL. 2002. *Physical Hydrology (Second Edition)*. Waveland Press, Inc.: Long Grove, Illinois, USA.

Ehsanzadeh E, Spence C, van der Kamp G, McConkey B. 2012. On the behaviour of dynamic contributing areas and flood frequency curves in North American Prairie watersheds. *Journal of Hydrology* **414-415**: 364–373. DOI: 10.1016/j.jhydrol.2011.11.007.

Environment Canada. 2012. National Climate Archive. http://climate.weatheroffice.gc.ca. Date accessed: 26 July 2014.

Euliss NH, LaBaugh, JW, Fredrickson LH, Mushet DM, Laubhan MK, Swanson GA, Winter TC, Rosenberry DO, Nelson RD. 2004. The wetland continuum: A conceptual framework for interpreting biological studies. *Wetlands* **24**(2): 448–458.

Fang X, Pomeroy J. 2008. Drought impacts on Canadian prairie wetland snow hydrology. *Hydrological Processes* **22**: 2858–2873. DOI: 10.1002/hyp.

Fang X, Pomeroy J. 2009. Modelling blowing snow redistribution to prairie wetlands. *Hydrological Processes* **23:** 2557–2569.

Fang X, Pomeroy JW, Westbrook CJ, Guo X, Minke AG, Brown T. 2010. Prediction of snowmelt derived streamflow in a wetland dominated prairie basin. *Hydrology and Earth System Sciences* **14**: 991–1006. DOI: 10.5194/hess-14-991-2010.

Ferone JM, Devito, KJ. 2004. Shallow groundwater–surface water interactions in pond–peatland complexes along a Boreal Plains topographic gradient. *Journal of Hydrology* **292**(1): 75-95.

Gleason RA, Euliss NH. 1998. Sedimentation of prairie wetlands. *Great Plains Research* **8:** 97–112.

Granger RJ, Gray DM, Dyck GE. 1984. Snowmelt infiltration to frozen Prairie soils. *Canadian Journal of Earth Sciences* **21**: 669–677.

Gray D, Landine P, Granger RJ 1985. Simulating infiltration into frozen prairie soils in streamflow models. *Canadian Journal of Earth Sciences* **22**: 464–472. DOI: 10.1139/e85-045.

Gray DM, Toth B, Zhao L, Pomeroy JW, Granger RJ. 2001. Estimating areal snowmelt infiltration into frozen soils. *Hydrological Processes* **15**: 3095–3111. DOI: 10.1002/hyp.320.

Guan XJ, Spence C, Westbrook CJ. 2010. Shallow soil moisture – ground thaw interactions and controls – Part 2: Influences of water and energy fluxes. *Hydrology and Earth System Sciences* **14**: 1387–1400. DOI:10.5194/hess-14-1387-2010.3

Harbaugh AW, Banta ER, Hill MC, McDonald MG. 2000. MODFLOW-2000, The US Geological Survey Modular Groundwater Model—User guide to modularization concepts and the groundwater flow process. *U.S. Geological Survey Open File Report, 00-92*.

Hayashi M, van der Kamp G. 2000. Simple equations to represent the volume–area–depth relations of shallow wetlands in small topographic depressions. *Journal of Hydrology* **237**: 74–85. DOI: 10.1016/S0022-1694(00)00300-0.

Hayashi M, van der Kamp G, Rudolph DL. 1998a. Water and solute transfer between a prairie wetland and adjacent uplands, 1. Water budget. *Journal of Hydrology* **207**: 42–55. DOI: 10.1016/S0022-1694(98)00098-5.

Hayashi M, van der Kamp G, Rudolph DL. 1998b. Water and solute transfer between a prairie wetland and adjacent uplands, 2. Chloride cycle. *Journal of Hydrology 207*: 56-67.

Hayashi M, van der Kamp G, Schmidt R. 2003. Focused infiltration of snowmelt water in partially frozen soil under small depressions. *Journal of Hydrology* **270:** 214–229.

Heron R, Woo M. 1978. Snowmelt computations for a high arctic site. In *Proceedings of the 35th Eastern Snow Conference*. Hanover, New Hampshire; 162–172.

Horst TW. 1997. A simple formula for attenuation of eddy fluxes measured with first order response scalar sensors. *Boundary Layer Meteorology* **94**: 517-520.

Huang S, Young C, Abdul-Aziz OI, Dahal D, Feng M, Liu, S. 2013. Simulating the water budget of a Prairie Potholes complex from LiDAR and hydrological models in North Dakota, USA. *Hydrological Sciences Journal* **58**: 1434-1444.

Jencso KG, McGlynn, BL. 2011. Hierarchical controls on runoff generation: Topographically driven hydrologic connectivity, geology, and vegetation. *Water Resources Research* **47(**11).

Jencso KG, McGlynn BL, Gooseff MN, Wondzell SM, Bencala KE, Marshall LA. 2009. Hydrologic connectivity between landscapes and streams: Transferring reach- and plot-scale understanding to the catchment scale. *Water Resources Research* **45**: W04428. DOI: 10.1029/2008WR007225.

Johnson WC, Werner B, Guntenspergen GR, Voldseth RA, Millett B, Naugle DE, Tulbure M, Carroll RWH, Tracy J, Olawsky C. 2010. Prairie wetland complexes as landscape functional units in a changing climate. *BioScience* **60:** 128–140.

Krasnostein AL, Oldham CE. 2004. Predicting wetland water storage. *Water Resources Research* **40:** W10203.

Kirkby MJ. 1996. The Scientific Nature of Geomorphology: Proceedings of the 27th Binghamton Symposium in Geomorphology. BL Rhoads, CE Thorn (eds). John Wiley & Sons: New York; 257–272.

LaBaugh, JW. 1987. Hydrology and chemistry of selected prairie wetlands in the Cottonwood Lake area, Stutsman Country, North Dakota, 1979-82. *US Geological Survey professional paper (USA).*

LaBaugh J, Winter TC, Rosenberry DO. 1998. Hydrologic functions of prairie wetlands. *Great Plains Research* **8:** 17–37.

LaBaugh JW, Winter TC, Swanson GA, Rosenberry DO, Nelson RD, Euliss NH. 1996. Changes in atmospheric patterns affect midcontinent wetlands sensitive to climate. *Limnology and Oceanography* **41**: 864–870.

Leibowitz S, Vining K. 2003. Temporal connectivity in a prairie pothole complex. *Wetlands* **23**(1): 13–25. DOI:10.1672/0277-5212(2003)023.

Lissey A. 1971. Depression-focused transient ground water flow patterns in Manitoba. *Geological Association of Canada Special Paper*.

Massman WJ. 2000. A simple method for estimating frequency response corrections for eddy covariance systems. *Agricultural and Forest Meteorology* **104**: 185-198.

McDonnell JJ. 2003. Where does water go when it rains? Moving beyond the variable source area concept of rainfall-runoff response. *Hydrological processes* **17(**9): 1869-1875.

McGlynn B, McDonnell JJ. 2003. Quantifying the relative contributions of riparian and hillslope zones to catchment runoff. *Water Resources Research* **39**(11): 1310. DOI: 10.1029/2003WR002091.

McNamara JP, Tetzlaff D, Bishop K, Soulsby C, Seyfried M, Peters NE, Aulenbach BT, Hooper R. 2011. Storage as a metric of catchment comparison. *Hydrological Processes* **25**: 3364–3371. DOI:10.1002/hyp.8113.

Mekonnen MA, Wheater HS, Ireson AM, Spence C, Davison B, Pietroniro A. 2014. Towards an improved land surface scheme for prairie landscapes. *Journal of Hydrology* **511**: 105-116.

Miller J, Acton D, Arnaud R. 1985. The effect of groundwater on soil formation in a morainal landscape in Saskatchewan. *Canadian Journal of Soil Science* **65**: 293–307. DOI: 10.4141/cjss85-033.

Minke AG, Westbrook CJ, van der Kamp G. 2010. Simplified volume-area-depth method for estimating water storage of Prairie potholes. *Wetlands* **30**: 541–551. DOI:10.1007/s13157-010-0044-8.

Nachshon U, Ireson AM, van der Kamp G, Davies SR, Wheater HS. 2014. Impacts of climate variability on wetland salinization in the North American Prairies, *Hydrology and Earth Systems Science* **10:** 13475-13503.

Oke TR. 1987. *Boundary layer climates*. Methuen: London; 435.

Parsons DF, Hayashi M, van der Kamp G. 2004. Infiltration and solute transport under a seasonal wetland: bromide tracer experiments in Saskatoon, Canada. *Hydrological Processes* **18**: 2011–2027. DOI:10.1002/hyp.1345.

Phillips RW, Spence C, Pomeroy JW. 2011. Connectivity and runoff dynamics in heterogeneous basins. *Hydrological Processes* **25**: 3061–3075. DOI:10.1002/hyp.8123.

Pomeroy JW, Gray, DM. 1995. Snow cover accumulation, relocation and management. NHRI Science Report.

Pomeroy JW, Gray DM, Brown T, Hedstrom NR, Quinton WL, Granger RJ, Carey SK. 2007. The cold regions hydrological model: a platform for basing process representation and model structure on physical evidence. *Hydrological Processes* **21**: 2650–2667.

Rodhe A. 1989. On the generation of stream runoff in till soils. *Nordic Hydrology* 20(1): 1-8.

Roulet, N. 1990. The hydrologic role of peat-covered wetlands. *Canadian Geographer* **34**: 82–83.

Seibert J, Bishop K, Nyberg L, Rodhe A. 2011. Water storage in a till catchment. I: Distributed modelling and relationship to runoff. *Hydrological Processes* **25**: 3937–3949. DOI: 10.1002/hyp.8309.

Seibert J, Bishop K, Rodhe A, McDonnell JJ. 2003. Groundwater dynamics along a hillslope: A test of the steady state hypothesis. *Water Resources Research* **39**(1): 1014. DOI: 10.1029/2002WR001404.

Shaw D, van der Kamp G, Conly FM, Pietroniro A, Martz L. 2012. The fill-spill hydrology of Prairie wetland complexes during drought and deluge. *Hydrological Processes* **26**(20): 3147–3156. DOI:10.1002/hyp.8390.

Shook K, Pomeroy J. 2012. Changes in the hydrological character of rainfall on the Canadian prairies. *Hydrological Processes* **26**: 1752–1766. DOI: 10.1002/hyp.9383.

Shook KR, Pomeroy JW. 2011. Memory effects of depressional storage in Northern Prairie hydrology. *Hydrological Processes* **25**: 3890–3898. DOI:10.1002/hyp.8381.

Sidle RC, Tsuboyama Y, Noguchi S, Hosoda I, Fujieda M, Shimizu T. 2000. Stormflow generation in steep forested headwaters: a linked hydrogeomorphic paradigm. *Hydrological Processes* **14**: 369–385.

Spence C. 2007. On the relation between dynamic storage and runoff: A discussion on thresholds, efficiency, and function. *Water Resources Research* **43**: W12416. DOI: 10.1029/2006WR005645.

Spence C. 2010. A paradigm shift in hydrology: Storage thresholds across scales influence catchment runoff generation. *Geography Compass* **4**(7): 819–833. DOI: 10.1111/j.1749-8198.2010.00341.x.

Spence C, Woo MK. 2003. Hydrology of subarctic Canadian shield: soil-filled valleys. Journal of Hydrology 279: 151-166. DOI: 10.1016/S0022-1694(03)00175-6.

Stewart RE, Kantrud KA. 1971. Classification of natural ponds and lakes in the glaciated prairie region. *US Department of the Interior, Fish & Wildlife Service Resource Publication 92*.

Su M, Stolte W, van der Kamp G. 2000. Modelling Canadian prairie wetland hydrology using a semi-distributed streamflow model. *Hydrological Processes* **14**: 2405–2422.

Todhunter PE, Rundquist BC. 2008. Pervasive wetland flooding in the glacial drift prairie of North Dakota (USA). *Natural Hazards* **46**: 73–88. DOI:10.1007/s11069-007-9182-6.

Townley LR, Turner JV, Barr AD, Trefry MG, Wright KD, Gailitis V, Harris CJ, Johnston CD. 1993. *Wetlands of the Swan Coastal Plain, vol. 3, Interaction Between Lakes, Wetlands and Unconfined Aquifers*. Water Authority of Western Australia, Perth.

Toyra J, Pietroniro A, Craymer M, Veronneau M. 2006. Evaluation of LiDAR-derived ground surface Digital Elevation Model (DEM) in low-relief regions: Case study on the Canadian Prairies. In *Hydroscan: Airborne laser mapping of hydrological features and resources*. Hopkinson C, Pietroniro A, Pomeroy JW (eds). Canadian Water Resources Association: Canada; 301-326.

Tromp-van Meerveld HJ, McDonnell JJ. 2006. Threshold relations in subsurface stormflow: 2. The fill and spill hypothesis. *Water Resources Research* **42**: W02411. DOI: 10.1029/2004WR003800.

Valk, AGVD. 2005. Water-level fluctuations in North American prairie wetlands. *Hydrobiologia* **539:** 171–188.

van der Kamp G, Hayashi M. 2009. Groundwater-wetland ecosystem interaction in the semiarid glaciated plains of North America. *Hydrogeology Journal* **17**: 203–214. DOI: 10.1007/s10040-008-0367-1.

van der Kamp G, Hayashi M, Gallen D. 2003. Comparing the hydrology of grassed and cultivated catchments in the semi-arid Canadian prairies. *Hydrological Processes* **17**: 559–575.

van der Valk A. 2005. Water-level fluctuations in North American prairie wetlands. *Hydrobiologia* **539**: 171–188. DOI: 10.1007/s10750-004-4866-3.

Vining K. 2002. *Simulation of Streamflow and Wetland Storage, Starkweather Coulee Subbasin, North Dakota, Water Years 1981-1998*. Bismarck, North Dakota. Retrieved from http://www.csa.com/partners/viewrecord.php?requester=gs&collection=TRD&recid=N0310820AH

Webb EK, Perman GI, Leuning R. 1980. Correction of flux measurements for density effects due to heat and water vapour transfer. *Quarterly Journal of the Royal Meteorological Society* **106**: 85–100.

Weiler M, McDonnell J. 2004. Virtual experiments: a new approach for improving process conceptualization in hillslope hydrology. *Journal of Hydrology* **285**: 3-18.

Winter TC. 1989. Hydrologic studies of wetlands in the northern prairie. In *Northern prairie wetlands*, A Valk (eds). Iowa State University Press: Ames, Iowa; 16-54.

Winter TC. 2000. The vulnerability of wetlands to climate change: a hydrologic landscape perspective. *Journal of the American Water Resources Association* **36(**2): 305-311.

Winter TC, Rosenberry DO. 1995. The interaction of ground water with prairie pothole wetlands in the Cottonwood Lake area, east-central North Dakota, 1979–1990. *Wetlands* **15:** 193–211.

Winter TC, Rosenberry DO. 1998. Hydrology of prairie pothole wetlands during drought and deluge: A 17-year study of the Cottonwood Lake wetland complex in North Dakota in the perspective of longer term measured and proxy hydrological records. *Climatic Change* **40**: 189–209.

Woo MK, Rowsell RD. 1993. Hydrology of a prairie slough. *Journal of Hydrology* **146**: 175–207. DOI: 10.1016/0022-1694(93)90275-E.

Woo MK, Sauriol J. 1981. Effects of snow jams on fluvial activities in the High Arctic. *Physical Geography* **2**: 83-98.

Yates TT, Si BC, Farrell RE, Pennock DJ. 2006. Probability distribution and spatial dependence of nitrous oxide emission: Temporal change in hummocky terrain. *Soil Science Society of America Journal* **70**: 753–762. DOI: 10.2136/sssaj2005.0214.

Zhao L, Gray DM. 1999. Estimating snowmelt infiltration into frozen soils. *Hydrological processes* **13**: 1827-1842.

Zhao L, Gray DM, Male DH. 1997. Numerical analysis of simultaneous heat and mass transfer during infiltration into frozen ground. *Journal of Hydrology* **200**: 345-363.